UNIVERSIDADE DE LISBOA
FACULDADE DE CIÊNCIAS
DEPARTAMENTO DE BIOLOGIA VEGETAL

PHOTOPROTECTION AND PHOTOINHIBITION IN THE DIATOM *PHAEODACTYLUM TRICORNUTUM*

Nuno Manuel Cardoso Domingues

DISSERTAÇÃO DE MESTRADO EM BIOLOGIA CELULAR E BIOTECNOLOGIA
2011

UNIVERSIDADE DE LISBOA
FACULDADE DE CIÊNCIAS
DEPARTAMENTO DE BIOLOGIA VEGETAL

PHOTOPROTECTION AND PHOTOINHIBITION IN THE DIATOM *PHAEODACTYLUM TRICORNUTUM*

Nuno Manuel Cardoso Domingues

Dissertation supervised by:

Prof. Dr. Jorge Marques da Silva (Departamento de Biologia Vegetal / BioFIG)

Dr. Paulo Cartaxana (Departamento de Biologia Vegetal / Centro de Oceanografia)

DISSERTAÇÃO DE MESTRADO EM BIOLOGIA CELULAR E BIOTECNOLOGIA
2011

… 'Eu adoro todas as coisas
E o meu coração é um albergue aberto toda a noite.
Tenho pela vida um interesse ávido
Que busca compreendê-la sentindo-a muito.
Amo tudo, animo tudo, empresto humanidade a tudo,
Aos homens e às pedras, às almas e às máquinas,
Para aumentar com isso a minha personalidade.

Pertenço a tudo para pertencer cada vez mais a mim próprio
E a minha ambição era trazer o universo ao colo
Como uma criança a quem a ama beija.
Eu amo todas as coisas, umas mais do que as outras,
Não nenhuma mais do que outra, mas sempre mais as que estou vendo
Do que as que vi ou verei.
Nada para mim é tão belo como o movimento e as sensações.
A vida é uma grande feira e tudo são barracas e saltimbancos.
Penso nisto, enterneço-me mas não sossego nunca.'…

Álvaro de Campos, excerto de *Acordar, in* 'Poemas'

AGRADECIMENTOS

Em primeiro lugar quero agradecer aos meus orientadores, Doutor Jorge Marques da Silva e Doutor Paulo Cartaxana, tanto pela oportunidade de desenvolver a tese de Mestrado neste projecto como pelo bom espírito. Foi verdadeiramente um prazer trabalhar convosco.

Um grande obrigado à Dona Manuela Lucas, sem a qual as coisas não teriam certamente corrido tão bem. A minha 'avózinha' do laboratório, embora mãezinha fosse um termo mais apropriado. Muito obrigado por toda a sua ajuda, os seus ensinamentos e por ser uma boa amiga. E por me ensinar que nem todas as plantas são aquáticas!

Doutora Ana Rita Matos, agradeço-lhe principalmente os seus conhecimentos em Biologia Molecular, todas as suas dicas e por me ajudar a ter western blots mais bonitos. Gostava que pudéssemos ter trabalhado juntos mais vezes.

Também quero agradecer ao Doutor João Arrabaça pelas boas vibrações, por partilhar os seus conhecimentos e me ajudar quando necessário.

Doutora Anabela Silva, vou agradecer-lhe especialmente pelas suas constantes e contagiantes boa disposição e simpatia. Obviamente também agradeço muito todas as vezes que me ajudou.

Mickael Ruivo, obrigado por toda a ajuda que deste para que eu soubesse como cultivar diatomáceas e por ofereceres ajuda sempre que precisasse. E tudo o resto, por seres um bom companheiro e dares boas dicas.

Rute Miguel e Teresa Granja, obrigado pela ajuda, o material que me emprestaram e as ocasionais companhias ao almoço.

Necessito também de agradecer a todas as outras pessoas da Faculdade que estiveram lá para mim de algum modo. Um grande obrigado para a Professora Doutora Filomena Caeiro, Célia Lima, Dave Pinxteren, João, Sónia Vieira, Vera Veloso, Ana Amorim, Marta Mendes e todas as outras pessoas que aqui não refiro.

Alejandro Olejua, obrigado por seres o meu melhor amigo, por toda a ajuda que me deste, incluindo discussões sobre trabalho, as conversas, por vires da Alemanha para o meu aniversário, por me possibilitares dizer que tenho um melhor amigo. Mais cara-metade. As saudades apertam às vezes, mas sei que estás aí algures e que nos vamos ver muitas vezes mais ao longo da vida. Provavelmente tiveste o maior impacto na minha vida de todas as pessoas que conheci até hoje. Boa sorte com o teu Doutoramento.

Andrea Rodrigues, outra grande amiga que foi para longe. Não devias ter ido para Edimburgo, mas na verdade devias e foste! Sabes que te amo, sabes que eu sou mais palerma contigo do que com qualquer outra pessoa. E sabes que sinto a tua falta. És a minha luz para perseguir as minhas ambições. O meu modelo para a vida. Gostava que estivesses aqui. Mas também quero ir aí ver como foi a tua mudança de vida. Muito obrigado por seres minha amiga e por tentares ensinar-me matemática a toda a hora, mesmo que com pouco sucesso. Desculpa pelo modo como fiz com que insistentemente nos tornássemos amigos. Não me arrependo nada obviamente, ainda bem que fui teimoso.

A grande Patrícia Serrano, que recentemente mostrou-me o que uma amizade pode ser, e que há pessoas que fazem coisas pelos amigos que nem me passariam pela cabeça (oito horas num hospital sem comida a fazer companhia, da boa claro, não é para toda a gente). Sofremos, passámos fome, doía-me tudo, mas essa noite está na minha cabeça como um belo episódio da minha vida, porque nessa noite apercebi-me que tinha outra grande pessoa na minha vida. Só te desejo coisas boas. E obviamente estarei sempre lá para ti do mesmo modo.

Ana Margarida Rodrigues, obrigado por estares sempre a insistir para escrever a tese, para me manter a par de ti. Claro que nunca o estive, visto que enquanto escrevo isto tu já estás praticamente despachada e eu não. Obrigado pela amizade e teimosia.

Joana Pereira, a minha mãe da mesma idade. És uma daquelas pessoas irritantemente preocupadas que fazem tudo por aqueles com quem se preocupam. Eu só desejo que sejas mais honesta contigo própria e que pudesses ser mais feliz. Agradeço-te profundamente todas as vezes que lá estiveste para mim. És outra amiga única.

Luísa Mota, uma das minhas amigas adultas. Estou só a brincar como sabes. Conheci-te há pouco tempo mas já tens um grande papel na minha vida. Fazes-me rir até quando falamos de coisas tristes. De algum modo a coisa vira-se e ganham piada. Ahhhhhh, é refrescante. Foste uma lufada de ar fresco na minha vida. És a minha sereia.

Obrigado Jorge Faria, por todas as gargalhadas, as conversas, a companhia, a ajuda… e as lavagens!

Todos os meus outros amigos que estiveram lá para mim de alguma maneira, a ajudarem-me como podiam, a serem boa companhia, a partilharem as suas experiências, ou simplesmente a fazer-me sorrir. Todas as outras pessoas que se cruzaram comigo e me deram algo novo. Citando alguns nomes, Joana Boavida, Tiago Gomes, Larissa Tura, Telma João Santos, Custódio Nunes, André Alcântara, Susana Silvestre, Carlos Silva, Alicja Gladysz, Marisa Nunes, Pa Pu, Elisabete Pessanha, Elsa Serra, Sofia Borges, Lurdes Vargas, etc. Com certeza não me terei lembrado de todos, mas aqui fica expressa a intenção.

O meu maior agradecimento vai para os meus pais. Mãe, tu és o ser vivo mais bonito à face da Terra. Dás tudo aos outros sem pedir nada em troca. Pai, és a pessoa mais trabalhadora que conheço e defendes os teus valores como ninguém. Mesmo que não concorde com eles por vezes, és suficientemente aberto à persuasão (dificilmente, mas a dinâmica deste teu comportamento até que tem o seu quê de interessante, quando não é demais). Ambos me ensinaram tanta coisa e deram-me a maior parte dos meus valores. Sem vocês não poderia ter acabado este Mestrado, viver em Lisboa e arrisco-me a dizer, ser feliz. Estou contente com a pessoa que sou hoje, sendo vocês os pilares da minha educação. Mas não só…

Ao meu irmão, à minha cunhada e ao meu sobrinho. João, és hoje em dia o grande irmão que nunca senti ter na infância. Cresceste (crescemos os dois) e cresceste bem. Tornaste-te uma grande pessoa e um grande pai. O mesmo se pode dizer em relação à Tânia. Admiro a vossa paternidade. E Tânia, a tua amizade sempre me fez feliz de imaginar que um dia serias a mulher do meu irmão. E deram-nos o Pedro, a quem tenho de agradecer por me deixar sempre com um grande sorriso na cara sempre que o vejo.

À minha avó. Pensas que estás sozinha agora, mas não estás. Obrigado por sempre teimosamente estares lá. És a melhor. Obrigado por todos os doces e bolos que me levavas e aos meus amigos à escola primária, pelos almoços infinitos, por me sufocares com comida, por todas estas coisas e mais.

Ao meu avô. Já não estás entre nós, mas definitivamente, és provavelmente a pessoa a quem devo mais que ninguém. Nunca to disse, mas és para mim uma grande pessoa, sempre dedicado à tua família, sempre lá para nós, sempre… Nem uma falha. Eras grande. Não eras perfeito, mas eras um grande homem e sempre fizeste tudo pelos teus filhos e netos. Obrigado por me ensinares a trabalhar com o torno mecânico, por me ensinares os básicos da condução, pelas histórias, pela calma, por me respeitares. Reconheço que estiveste lá para mim mais do que qualquer outra pessoa. Fazes falta e sempre farás.

ABBREVIATIONS

$^1O_2$ – singlet oxygen
3-PGA - 3-phosphoglyceric acid
a.u. – arbitrary units
ANOVA – analysis of variance
ATP – adenosine triphosphate
BSA – bovine serum albumine
CAB – chlorophyll *a*/*b* – binding proteins
$CaMn_4$ – manganese calcium cluster
Chl - chlorophyll
CO_2 – carbon dioxide
CP43 – core light-harvesting complex protein (43 kDa)
CP47 - core light-harvesting complex protein (47 kDa)
CtpA – carboxyl-terminal peptidase A
Cyt b_{559} – cytochrome b_{559}
Cyt b_6f – cytochromes b_6 and *f* complex
D1 – reaction centre D1 protein
D2 – reaction centre D2 protein
DD – diadinoxanthin
DegP/Htr – degrade periplasmic proteins/high temperature requirement ATP-independent serine endoproteases
DES – de-epoxidation state
DHAP – dihydroxyacetone phosphate
DT - diatoxanthin
DTT - dithiothreitol
e^- - electron
H^+ - hydrogen proton
E - ambient spectrally averaged photon irradiance of PAR (400–700 nm)
EDTA - ethylenediaminetetraacetic acid
E*k* - light-saturation parameter of the ETR versus E curve (µmol photons.m^{-2}.s^{-1})
ELIPS – early-light induced proteins
rETR – relative electron transport rate (dimensionless)
$rETR_m$ – maximum relative electron transport rate in the E versus ETR curve (dimensionless)
F_0 – minimum fluorescence of dark-adapted chloroplasts
F_0' – minimum fluorescence of light-adapted chloroplasts
FCP/ fcp – fucoxanthin-chl *a*-chl *c* – binding proteins
Fd - ferredoxin
FDN – ferredoxin/$NADP^+$ reductase complex
Fig. - figure
F_m – maximum fluorescence of dark-adapted chloroplasts
F_m' - maximum fluorescence of light-adapted chloroplasts
FtsH – filamentation temperature sensitive H ATP-dependent zinc-metalloprotease
F_v – variable fluorescence ($F_m - F_0$ or $F_m' - F_0'$)
F_v/F_m – Quantum yield of dark-adapted chloroplasts (dimensionless)
F_v'/F_m' - Quantum yield of light-adapted chloroplasts (dimensionless)
g – standard gravity or standard acceleration due to free fall
h - hour
H_2O – water
H_2O_2 – hydrogen peroxide
HCl – chloridric acid
HL – high light
HLi – high light with inhibitor (lincomycin)
HLIPS – high-light induced proteins
HPLC – high performance liquid chromatography
HRP – horse-radish peroxidase
iC – inorganic carbon
L - litre
Lhc - light harvesting complex genes
LHC – light-harvesting complex proteins
LL – low light

LLi – low light with inhibitor (lincomycin)
MAD – malondialdehyde
mAU – milli absorbance units
min - minute
Na_2HPO_4 – disodium hydrogen phosphate
NaCl – sodium chloride
$NADP^+$ - nicotinamide adenine dinucleotide phosphate
NADPH – reduced nicotinamide adenine dinucleotide phosphate
NaH_2PO_4 – sodium phosphate
$NaHCO_3$ – sodium bicarbonate
NPQ – non-photochemical quenching
O_2 – di-oxygen
O_2^- – superoxide anion
OEC – oxygen-evolving complex
P – power of statystical test
P680 – photosystem II primary donor (absorbs mainly at 680 nm)
PAM – pulse-amplitude modulated
PAR – photosynthetically available radiation
PBS-T – phosphate buffer saline with tween-20
pD1 – percursor D1 protein
P_{max} – photon-saturated photosynthetic rate
PMSF - phenylmethylsulfonyl fluoride
pQ – photochemical quenching
PQ – plastoquinone
PS - photosystem
psbA,B,C,D,S / *psbA,B,C,D,S* – photosystem II D1, CP47, CP43, D2, psbS proteins/genes
Q - quencher
Q_A – plastoquinone (quencher A), first acceptor plastoquinone
Q_B – plastoquinone (quencher B), second acceptor plastoquinone
q_E - energy quenching, rapidly reversible component of NPQ
q_I - photoinhibitory quenching, slowly reversible component of NPQ
RLC – rapid light curve (rapid ETR versus E curve)
ROS – reactive oxygen species
s - second
s.d. – standard deviation of the mean
SCPs – small cab-like proteins
SDS-PAGE – sodium dodecyl-sulfate polyacrylamide gel electrophoresis
cpSec – chloroplast general secretory pathway translocase system
Tris – tris buffer saline
Tween 20 – polysorbate 20 surfactant
UV - ultraviolet
α – significance level of statistical test
α / β - initial slope indicative of photosynthetic efficiency /photoinhibition parameter of the ETR versus E curve
Φ_{PSII} - quantum yield of photosystem II
mL – millilitre (10^{-3} litres)
RuBP – ribulose-1,5-bisphosphate
µg – microgram (10^{-6} grams)
µL – microlitre (10^{-6} litres)
µmol – micromol (10^{-6} moles)
nm – nanometer (10^{-9} meters)
fmol – femtomol (10^{-15} mol)
mol – mole (6.02×10^{23} elementary entities)
pg – picogram (10^{-12} grams)
pmol – picomol (10^{-12} mol)

ABSTRACT

Productivity in marine environments is largely based on the photosynthetic activity of diatoms, microalgae that account for ca. 40% of global oceanic carbon fixation. High photosynthetic rates in diatoms are maintained despite the systematic exposure to changing environmental conditions. Of particular importance is the exposure to changing irradiances, including supersaturating light levels. The success of diatoms in coping with high light has been attributed to the efficiency of their photoprotective mechanisms. In this study, we investigated the effect of light stress on the reaction centre protein D1/psbA from photosystem II of *Phaeodactylum tricornutum*, which has been shown to be the major target of photodamage. Cultures were grown at 40 µmol photons.m^{-2}.s^{-1} (used as control) and subjected to 1 h high light (HL) stress of 1,250 µmol photons.m^{-2}.s^{-1}. Lincomycin was added to half of the cultures to infer on PSII repair capacities, by determining D1 concentration with immunoblotting. Pulse-amplitude modulated fluorometry was used to measure stress effects on quantum yield and non-photochemical quenching (NPQ). Pigment concentrations, including the xanthophylls diadinoxanthin and diatoxanthin, were quantified by High Performance Liquid Chromatography (HPLC). It was observed a decrease in D1 in both light treatments, but much more pronounced in HL. Lincomycin affected D1 repair, particularly in HL where almost no D1 was detected. Quantum yield of PSII decreases after 1 h of HL, recovering almost 50%, while lincomycin treated cultures only recovered 25%. NPQ was similar in both treatments, reaching a maximum of 5.7, with diatoxanthin increasing under HL. NPQ's energy-dependent quenching (qE) dissipated after 13-20 min, while photoinhibitory quenching (qI) was still present after 24 h of recovery. Rapid light curves (RLCs) show a decrease in α, a maintained $rETR_m$ which decreases only in lincomycin treated cultures and an increased E*k* when lincomycin is added, although it is decreased after recovery. D1 degradation has a damaging effect on PSII repair and recovery, supported by the lowered quantum yields and the high NPQ. *P. tricornutum* therefore seems to have highly efficient photoprotective mechanisms, with photoinhibition occurring only when repair cannot keep up with the damage inflicted, which was only observed in HL.

KEYWORDS: D1/PsbA, photosystem II, *Phaeodactylum tricornutum*, quantum yield, photoprotection, photoinhibition.

RESUMO

Numa altura em que as alterações climáticas se tornaram a prioridade em termos de sustentabilidade do planeta, a atenção para com organismos com particular importância para a fixação de carbono é essencial. O fitoplâncton é responsável por quase 50 % da fixação de carbono inorgânico na Terra, sendo necessária uma percepção mais aprofundada do seu papel nos ecossistemas, e o seu impacto global, que até há umas décadas atrás era ainda largamente ignorado. A produtividade nos ecossistemas marinhos é maioritariamente baseada na actividade de diatomáceas (Baccillariophyceae), microalgas que habitam todo o tipo de ambientes aquáticos, responsáveis por cerca de 40 % da fixação de carbono pelos oceanos, quase 25 % a nível global. São um grupo de organismos extremamente diverso, com cerca de 200,000 espécies descritas, e os seus cloroplastos envoltos por duas membranas, resultado de uma hipotética endossimbiose secundária, evoluindo da linhagem vermelha de cloroplastos. A sua parede celular de sílica, denominada frústula, é formada por duas partes assimétricas, daí o nome do grupo. Possuem altas taxas fotossintéticas, que são mantidas apesar da exposição sistemática a condições ambientais variáveis, sendo por isso de relevo o seu papel nos ecossistemas, como moduladores do ciclo do silício devido às suas frústulas de sílica, que também as tornam promissoras no campo da nanotecnologia, bem como a sua aplicação na indústria dos biocombustíveis, devido ao seu alto teor em lípidos, que as torna bastante promissoras para a produção de *biodiesel*. Relativamente às dificuldades por que passam as diatomáceas nos seus habitats, é de salientar a exposição a diferentes irradiâncias, incluindo níveis saturantes de luz. O sucesso das diatomáceas em lidar com luz elevada tem sido atribuído à eficiência dos seus mecanismos fotoprotectores. Os organismos fotossintéticos têm também mecanismos de reparação quando os seus aparelhos fotossintéticos são danificados. No entanto, se os danos infligidos por um qualquer tipo de stresse forem demasiado fortes, de modo que a reparação não acompanhe, ou seja mesmo inibida, ocorre inibição da fotossíntese. Esta, caso seja provocada pelo excesso de luz, designa-se de fotoinibição. O excesso de luz reflecte-se na degradação de proteínas que constituem o fotossistema II (PSII), principalmente da proteína D1/psbA, que é desfosforilada e degradada pela protease FtsH nas membranas tilacoidais em contacto com o estroma dos cloroplastos. A fotoinibição pode provir do lado dos dadores ou aceitadores de electrões (e^-), em que vários constituintes ou envolventes do PSII provocam danos directos nos constituintes do PSII, ou produzem intermediários responsáveis pela formação de espécies reactivas de oxigénio

(ROS), que vão actuar principalmente na reparação de proteínas, por inibição da sua tradução. Para tal os organismos desenvolveram mecanismos para se protegerem destes fenómenos prejudiciais, produzindo anti-oxidantes como a superóxido dismutase, peroxidase ou o α-tocoferol, e pigmentos que dissipam a energia em excesso, como carotenóides, dos quais se salientam as xantofilas, cujo mecanismo de de-epoxidação produz pigmentos extremamente poderosos na dissipação de energia na forma de calor, o chamado *quenching* não-fotoquímico (NPQ). Neste estudo investigámos o efeito de stress luminoso na proteína D1/PsbA, pertencente ao centro de reacção do PSII, em *Phaeodactylum tricornutum*, proteína que está provada ser o alvo principal de danos causados pela luz. Para tal, fizeram-se crescer culturas a 40 µmol fotões.m^{-2}.s^{-1} (usadas como controlo) e algumas foram sujeitadas a 1 h de stress de luz alta a 1,250 µmol fotões.m^{-2}.s^{-1}. Um inibidor da síntese de proteínas de cloroplastos, lincomicina, foi adicionado a metade das culturas de cada tratamento, para determinar a capacidade de reparação da proteína e o efeito na actividade fotossintética. Determinou-se a concentração de D1 com recurso a *western immunoblotting*, utilizando-se anticorpos anti-psbA e um anticorpo secundário conjugado com *horse-radish* peroxidase (HRP), concretizando-se a quantificação absoluta calibrando com proteína D1 purificada. A fluorometria de Pulso Modulado (PAM) foi usada para determinar o rendimento quântico do fotossistema II antes, durante e após irradiância com luz alta, e após 24 h de recuperação no escuro, e ainda os mecanismos de fotoprotecção. Esta técnica baseia-se na emissão de fluorescência pela clorofila *a*, um modo de dissipação de energia quando esta não é transformada em energia fotoquímica, ou seja, quando os fotões que são absorvidos pela clorofila não induzem a doação de um electrão ao primeiro aceitador de e^-, a feofitina (Pheo), passando pela Tyr_Z^+. Nestas situações os centros de reacção dizem-se fechados e a energia dos fotões é reemitida como fluorescência, ou como calor (NPQ). Foram ainda efectuadas curvas rápidas de luz (RLC) para se obter a eficiência fotossintética (α), o transporte máximo de electrões relativo ($rETR_m$) e o coeficiente de saturação de luz, isto é, a luz a que o ETR é máximo (E*k*). As concentrações de pigmentos, incluindo das xantofilas diadinoxantina (DD) e diatoxantina (DT), foram determinadas através de Cromatografia Líquida de Alta Performance (HPLC). Pretendia-se confirmar a de-epoxidação de DD em DT pela enzima DD de-epoxidase, verificar diferenças significativas entre estes dois pigmentos, e possíveis alterações no teor de clorofila *a* ou dos outros pigmentos, como a fucoxantina e a clorofila *c*, e a concentração de β-caroteno, também responsável pela dissipação de energia em excesso. Observou-se uma diminuição em D1 em todos os tratamentos, mas muito mais pronunciada em luz alta. A lincomicina afectou a reparação de D1, particularmente em luz alta onde quase

não se detectou D1. O rendimento quântico do PSII obtido durante a incidência de luz alta foi praticamente nulo, e 24 h após se desligar a luz alta, recuperou quase 50 %, enquanto as culturas com lincomicina apenas recuperaram 25 %. O NPQ foi semelhante em ambos os tratamentos, atingindo um máximo de 5.7, com a diatoxantina a aumentar durante a incidência de luz alta, diminuindo após as culturas serem de novo colocadas no escuro. Todos os outros pigmentos mantiveram-se constantes em todos os tratamentos. Um dos componentes do NPQ, o *quenching* dependente de energia (qE), dissipou-se após 13-20 min, enquanto o *quenching* fotoinibitório (qI) observou-se ainda após 24 h de recuperação no escuro. As RLCs sugerem um decréscimo na eficiência da fotossíntese após a recuperação, mas uma manutenção do $rETR_m$, que decresce apenas nas culturas tratadas com lincomicina. Inesperadamente, o E*k* aumentou 40 min após se adicionar lincomicina, antes de se irradiar as culturas com luz alta, embora decresça após a recuperação do stress. Os resultados obtidos sugerem que os elevados níveis de degradação de D1, particularmente em HL, têm um efeito destrutivo na reparação e recuperação do fotossistema II, comprovado pela diminuição do rendimento quântico após irradiação com luz alta e pelo elevado NPQ possibilitado pela conversão e síntese *de novo* de diatoxantina, que dissipa a energia dos centros de reacção saturados de luz. *P. tricornutum* parece, por tudo isto, ter mecanismos protectores muito eficientes, e apesar de ocorrer fotoinibição, isto é, danos irreversíveis, estes só ocorrem quando a reparação do fotossistema II, nomeadamente da proteína D1, não é efectuada ao mesmo ritmo que os danos causados, o que só foi observado em condições de luz alta. Sendo assim, embora ocorra fotoinibição quando irradiados 1,250 µmol fotões.m^{-2}.s^{-1}, a reparação do PSII resulta numa eficiente capacidade de recuperação por parte desta diatomácea. Em trabalhos posteriores seria interessante medir o teor em ROS, para determinar influência do stress oxidativo, bem como apoiar o estudo com a análise também ao nível dos transcritos, quer seja de transcritos da D1, como de outras proteínas do PSII como a D2 ou a CP43, que embora não à mesma escala, também se sabe serem bastante degradadas em algumas diatomáceas.

PALAVRAS-CHAVE: D1/PsbA, fotossistema II, *Phaeodactylum tricornutum*, rendimento quântico, fotoprotecção, fotoinibição.

INDEX

INTRODUCTION

Microscopic autotrophic organisms greatly contribute to carbon fixation, when compared to more complex organisms. The unicellular character and relative small cell size facilitates nutrient uptake, metabolism and regeneration rates (Falkowski and Raven, 1997). Thus, they have a much more productive metabolism than multicellular autotrophs, being able to perform photosynthesis with a minimal waste of energy (Bowler et al., 2009). Carbon fixation is therefore much more efficient in phytoplankton than in macroalgae and plants. Phytoplankton in the ocean is responsible for almost 50% of total global carbon fixation (Armbrust et al., 2004; Nymark et al., 2009; Siaut et al., 2007), 40% of which corresponds to the Baccillariophyceae diatoms alone (Armbrust, 2009; Bozarth et al., 2009; Falkowski et al., 2004; Siaut et al., 2007).

The diatoms (Baccillariophyceae)

The name of this particular group of organisms comes from the greek *diatomos*, meaning 'cut in half', due to the two separated and assymetrical parts of the silica cell walls, or frustules (Armbrust, 2009). In what relates to their symmetry, they can be centric or pennate, belonging respectively to the orders Centrales or Pennales (Bertrand, 2010). They inhabit waters all over the world, as long as there are the necessary nutrients and light (Armbrust, 2009; Siaut et al., 2007), possibly being the most successful and diverse group of unicellular photosynthetic eukaryotes, with an estimated 200,000 different species (Siaut et al., 2007). Cyanobacteria are actually the most abundant autotrophs in the oceans (Falkowski et al., 2004), and presumably the ancestor of the more modern eukaryotic forms, as defended by the endosymbiotic hypothesis stating that a coccoid cyanobacterium became a membrane-bound plastid after being engulfed by an eukaryotic cell (Falkowski et al., 2004). From here on, eukaryotic forms diverged into a green lineage, which gave rise to green algae and land plants, and a red lineage, which spread from red algae (Falkowski et al., 2004). A secondary endosymbiosis occurring by engulfment of a red algae by a heterotroph and maybe a green algae as well (Armbrust, 2009), gave rise to groups such as some dinoflagellates,

coccolitophorids and the diatoms. The evolved forms of this latter symbiosis, with particular emphasis on diatoms, are much more diverse, presumably due to higher plastid portability, and represent the major producers in aquatic environments, particularly in oceanic turbulent waters and in coastal zones where upwelling occurs (Armbrust, 2009; Falkowski et al., 2004; Lavaud et al., 2007a; Materna et al., 2009). The global silica cycle is controlled largely by their silica frustules (Armbrust, 2009), which deposit in ocean basins after death. The frustules intricate architecture is also a prominent research interest in nanotechnology. Diatoms high lipid contents make them particularly attractive for engineering and production of biodiesel (Anemaet et al., 2010; Greenwell et al., 2010; Halim et al., 2011).

Although they constitute a major part of phytoplankton, some of them are actually benthonic, living on the surface of sediments (Cartaxana and Serôdio, 2008). Microscopic autotrophic benthos (microphytobenthos) is normally constituted mainly by different species of diatoms. Photosynthetic aquatic organisms can be subjected to high irradiances, especially in habitats like intertidal areas, where they need to deal with periods of high light irradiance during low tide. If photosynthesis is impaired, photoinhibition is said to occur. *Phaeodactylum tricornutum* is a model pennate diatom species, widely used, due to its ease of culture and fast growth rates. Although it is mainly planktonic, it can also be found in benthic communities in fine muddy or sandy sediments (epipelic), particularly in intertidal areas. Its genome has already been sequenced and it is therefore one of the most studied organisms in molecular aspects of photosynthesis.

Photosynthesis in aquatic environments

Although oxygenic photosynthesis is maintained largely unchanged in all photoautotrophs, there are differences that can be observed particularly in aquatic environments, where light quality and quantity, temperature and nutrient availability are the main variables (Zehr and Kudela, 2009). In the water, light isn't transmitted as in the air. It is scattered at a higher degree as a result of the particles and molecules in the water that change the refractive index in every inch of water (Falkowsky and Raven, 1997). Shorter wavelengths are sent back to the atmosphere and thus we see the water blue or green. Therefore, aquatic photoautotrophs have a huge diversity in pigment contents, whereas in higher plants the major pigment is always chlorophyll *a*. The diffusion of CO_2 in water is also

decreased four orders in magnitude when compared to the air, and other forms of inorganic carbon (iC) such as bicarbonate and carbonate anions are more abundant, except in more acidic waters where pH favors the CO_2 form. Therefore phytoplankton normally have mechanisms that favor acquisition of inorganic carbon when it is limited in solution, and in fact, it does not seem that iC is a limiting factor in oceans, except in some organisms (Falkowsky and Raven, 1997). These conditions created a truly diversified pool of adaptations in aquatic autotrophs, with changes to the photosynthetic apparatus that did not happen in terrestrial plants, as they have a common ancestor and had not as much diversification as algae.

The molecular architecture and physiology of the photosynthetic machinery

The photosynthetic apparatus is composed by two photosystems. PSII produces an oxidant strong enough to oxidize water and the electrons from water travel to PSI, where a reductant that has the capacity to reduce carbon dioxide is produced (NADPH). The photosynthetic chain is a set of pigment and protein complexes that act as light gatherers, the energy of which provides charge separation in reaction centres to subsequent acceptors and donors of electrons (Barber and Kuhlbrandt, 1999; Finazzi et al., 2003; Nelson and Yocum, 2006). Light-harvesting pigment-protein complexes (LHCs), the antennae, absorb light mainly with chlorophyll *a* (the primary electron donor, P680) and direct it to the reaction centre of photosystem II, where the excitation energy of light is converted to photochemical energy, by directing an electron through pheophytin (Pheo, the primary electron acceptor) to plastoquinone (Q_A), the first acceptor plastoquinone (Falkowski and Raven, 1997; Klimov and Baranov, 2001; Sarvikas et al., 2010). The electron originated from the photolysis of water by the oxygen evolving complex (OEC) is transferred to the chlorophyll molecule to regenerate it (Barber, 2008; Pantazis et al., 2009; Renger, 2001). From here on, an electron is transferred from donor to acceptor until it reaches the reaction centre of photosystem I, also coupled to LHCs that transmit the excitation energy of light needed for a new charge separation and continuation of electron transfer. Both reaction centres may have different pigment compositions, necessitating different action spectra. In the end, each electron is used to reduce $NADP^+$ to NADPH, by a ferredoxin/$NADP^+$ reductase complex. NADPH will be used in the dark reactions of the Calvin cycle. The movement of electrons along the chain also

causes a proton gradient across the chloroplast membrane, which is used by ATP synthase to generate ATP.

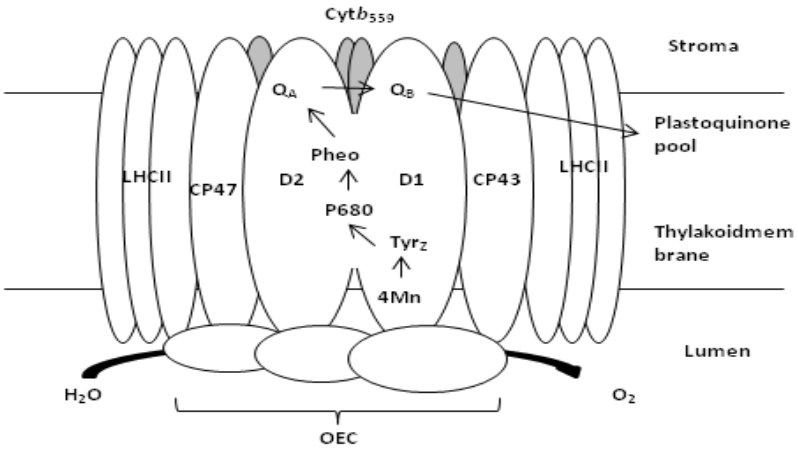

Figure 1 – Photosystem II architecture in thylakoid membranes, with reaction centres associated with the OEC and LHCII proteins, completed with electron trajectory (arrows). Cyt b_{559} – cytochrome b_{559}; LHCII – light-harvesting complex II protein-pigment complexes; 4Mn – calcium manganese cluster associated with OEC- oxygen evolving complex; P680 – primary donor chlorophyll *a*; Q_A – first acceptor plastoquinone; Q_B – second acceptor plastoquinone; Tyr_Z – immediate electron donor tyrosine, from 4Mn to P680, in D1. D1, D2, CP43 and CP47 are proteins from the reaction centre. Adapted from Yamamoto et al. (2008).

The reaction centre of photosystem II is composed by a heterodimer of the D1 protein (coded by the *psbA* gene) and D2 (*psbD*), which constitute the core (see Sharma et al., 1997 for detailed structure). These bind chlorophyll, pheophytin and plastoquinone co-factors involved in charge separation (Nixon et al., 2010), induced by the light absorbed by the antennae. In either side CP43 (*psbC*) and CP47 (*psbB*) bind several Chl *a* and β-carotenes. CP43 also participates in the ligation of $CaMn_4$ cluster that oxidizes water. CP43 and CP47 are highly conserved light-harvesting chlorophyll-protein complexes, and are said to be the core (or inner) antennae, normally connected to peripheral pigment-protein complexes that have accessory pigments, called LHCII or I(coded by the *LhcII* and *LhcI* genes, respectively), depending on which photosystem they are connected to. In higher plants and green algae these proteins are designated CAB proteins, for Chl *a*/*b*- binding proteins (Lang and Kroth,

2001). In diatoms these genes are designated *Fcp*, for fucoxanthin-Chl a-Chl *c*2 protein-complexes, or FCPs (Bertrand, 2010; Lang and Kroth, 2001).These accessory LHC proteins are encoded by nuclear genes, where mutations occur more frequently and recombination may occur, explaining the diversified nature of accessory LHCs as opposed to the core LHCs or the reaction centre proteins, which are chloroplast encoded. The accessory pigments such as β-carotene and xanthophylls are involved in excess light dissipation. In diatoms this architecture is maintained and accessory antennae are mainly bound to pigments such as fucoxanthin and chlorophyll *c*2. Among the various situations that can conduct to the failing of photosystems' normal function, is the production of reactive oxygen species (ROS), which are always produced, but more so when other physiological parameters are outside optimum levels, such as too much light that leads to photodamage.

Protective mechanisms against photoinhibition

Light is a major factor when referring to photosynthesis. Low light can be insufficient for efficient carbon assimilation, but too much PAR or UV radiation can also damage the pigment-protein complexes and subsequently decrease the efficiency and the potential of the photosynthetic machinery. It is important to take notice that photodamage occurs at all intensities of light (Aro et al., 2005). As electron transport is hindered, ROS are produced by electrons that leak from the chain and are free to react with oxygen species to produce singlet oxygen ($^1O_2$), hydrogen peroxide (H_2O_2) and the superoxide anion ($O_2^{\cdot -}$), which change protein conformations and damage membranes of cells and organelles. ROS formation can cause PSII acceptor or donor-side photoinhibition. On the donor-side, electron transfer from Tyr_Z^+ to $P680^+$ is interrupted and the highly oxidizing $P680^+$ or Tyr_Z^+ can lead to oxidation of nearby molecules such as pigments and amino acids or produce ROS such as superoxide (Napiwotzki et al., 1997). $P680^+$ appears to be the main cause of direct damage to the reaction centre D1 protein under normal light conditions (Yamamoto, 2001). On acceptor-side photoinactivation, the primary electron acceptor $Pheo^-$ recombination with $P680^+$can generate triplet P680, which reacting with oxygen, generates $^1O_2$ (Yamamoto et al., 2008). This happens by excessive reduction of Q_A reversing electron flow, or by charge recombination between the donor and acceptor sides (Murata et al., 2007). If Q_A is double reduced to Q_A^{2-} or stabilized by protonation (Q_AH_2), photosynthesis is also inhibited (Sarvikas et al., 2010).

Electrons can also leak when transferred from the secondary acceptor plastoquinone Q_B to the bulk plastoquinones, originating $O_2^{\cdot -}$ (Yamamoto et al., 2008). These ROS will damage the components of PS II, mainly the D1 protein. When light is not in excess, there is no accumulation of damaged PSII reaction centres, as there is a repair mechanism that fixes the damage (fig. 2). The repair mechanism is affected by higher intensities of light and other stressful events, and if repair cannot keep up with the damage inflicted at a given saturation point of irradiance where photosynthetic rates decline (P_{max}), photoinhibition occurs (Takahashi and Murata, 2008). The primary target of photodamage is the OEC, particularly the Mn cluster (Murata et al., 2007). These authors describe destruction of the Mn cluster of the OEC as being light-dependent and that the reaction centre D1 is inactivated by light absorbed by chlorophyll, being clear that ROS accelerate photoinhibition by inhibiting repair mechanisms (Edelman and Mattoo, 2008; Murata et al., 2007; Takahashi and Murata, 2008). In fact, several studies reveal that the repair of photosystem II is more sensitive to other environmental stresses than photodamage.

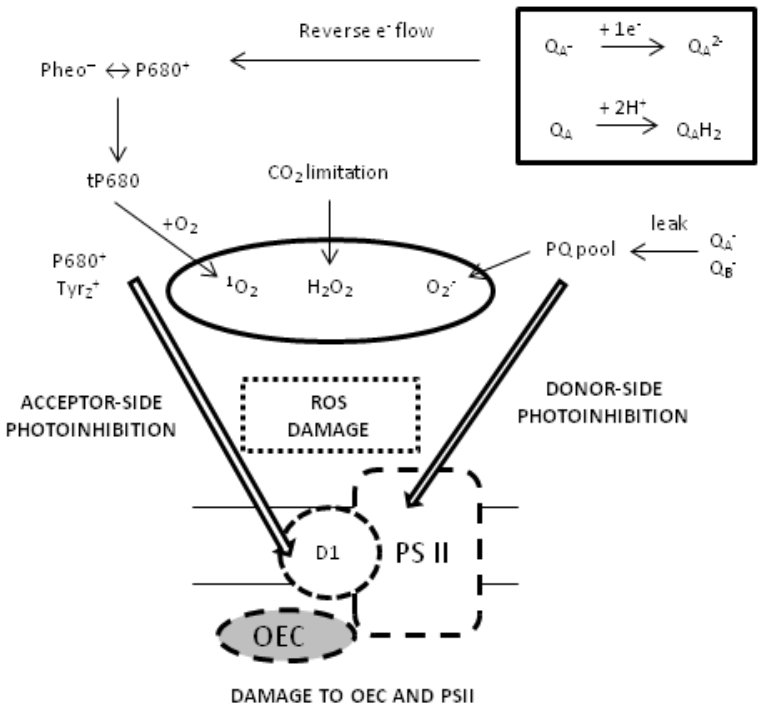

Figure 2 – Mechanisms of ROS production and damage to PS II by acceptor and donor-side photoinhibition.

When suffering photodamage, as to protect themselves from photoinhibition, photoautotrophic organisms developed different types of mechanisms. Constitutive pigments such as carotenes and xanthophylls can provide extra photons to chlorophylls or provide energy dissipation as heat (non-photochemical quenching, NPQ), away from over-excited chlorophylls, to avoid formation of triplet chlorophyll that can react with molecular oxygen and produce singlet oxygen (Depka et al., 1998). Xanthophylls are also thought to maintain membrane function, acting as stabilizers and making membranes impermeable to O_2 to avoid further formation of ROS (Ruban and Johnson, 2010). Other mechanisms are the existence of scavengers which reduce the ROS, negative phototaxis, secondary LHCs (CAB proteins and FCPs) and other special proteins synthesized called SCPs (small CAB-like proteins), such as ELIPS (early-light induced proteins) in higher plants, ferns and algae (Montane and Kloppstech, 2000) , HLIPS (high-light induced proteins) in cyanobacteria (Kilian et al., 2008; Nixon et al., 2010) and PsbS, only in higher plants (Bertrand, 2010; Montane and Kloppstech, 2000; Zhu and Green, 2010), which also act as pigment carriers for energy dissipation and reducing oxidative stress. Orthologs of the latter two haven't been found in algae (Bertrand, 2010; Nixon et al., 2010). When light starts to affect photosynthetic function more profoundly, the xanthophyll cycle comes into play, providing extra NPQ (Pieters et al., 2003; Ruban and Johnson, 2010). In this cycle, an epoxidized xanthophyll, diadinoxanthin (DD) in diatoms, is de-epoxidized by a de-epoxidase into diatoxanthin (DT), which will act as a quencher. These mechanisms that change the composition of LHCs, by relocating them and redistributing excitation energy among photosystems (Bonardi et al., 2005; Horton and Ruban, 2005), plus enzymes' translation, stimulated by signals that change transduction patterns of genomes, all provide further photoprotection (Walters, 2005). In diatoms such as *Phaeodactylum tricornutum*, NPQ levels are frequently five times larger than in higher plants (Nymark et al., 2009; Ruban and Johnson, 2010).

If organisms are exposed for a long period of time to high light, to a point where they adapt physiologically within their genetic potential limits and environmental constraints, they are said to be photoacclimated. If these photoprotection and photoacclimation processes aren't enough to prevent irreversible damage, chronic photoinhibition occurs (Nixon et al., 2010). As mentioned before, the major protein affected by photodamage and mostly connected to photoinhibition, has been shown to be the reaction centre protein D1/psbA (Aro et al., 2005; Depka et al., 1998; Kettunen et al., 1991; Nixon et al., 2010; Ohira et al., 2005; Pieters et al., 2003).

Repair during photodamage: D1 dynamics

D1 has been shown numerous times in literature to be the major protein affected by light damage in PSII, but a quick and efficient turnover mechanism keeps photosynthesis functioning. Its high rate of synthesis and turnover is a result of its constant activity, as D1 suffers frequently oxidative damage when catalyzing electron transfer from water to plastoquinone through the Mn cluster (Edelman and Mattoo, 2008; Krieger-Liszkay, 2005; Lindahl et al., 2000), besides negatively affected repair by over production of ROS. If too much light afflicts cells, the repair cycle cannot keep up with the damage inflicted, and photoinhibition will occur. The way the repair is conducted, even at low light intensities, remains largely unresolved, but evidence suggests that D1 is targeted for degradation by a signal, and translation of new D1 polypeptides is initiated. The precursor D1 (pD1) polypeptides are targeted to the damaged complexes where they substitute the degraded D1 (Nixon et al., 2010). Elimination and substitution of D1 into membrane bound PSII is thought to happen as shown in Fig. 3.

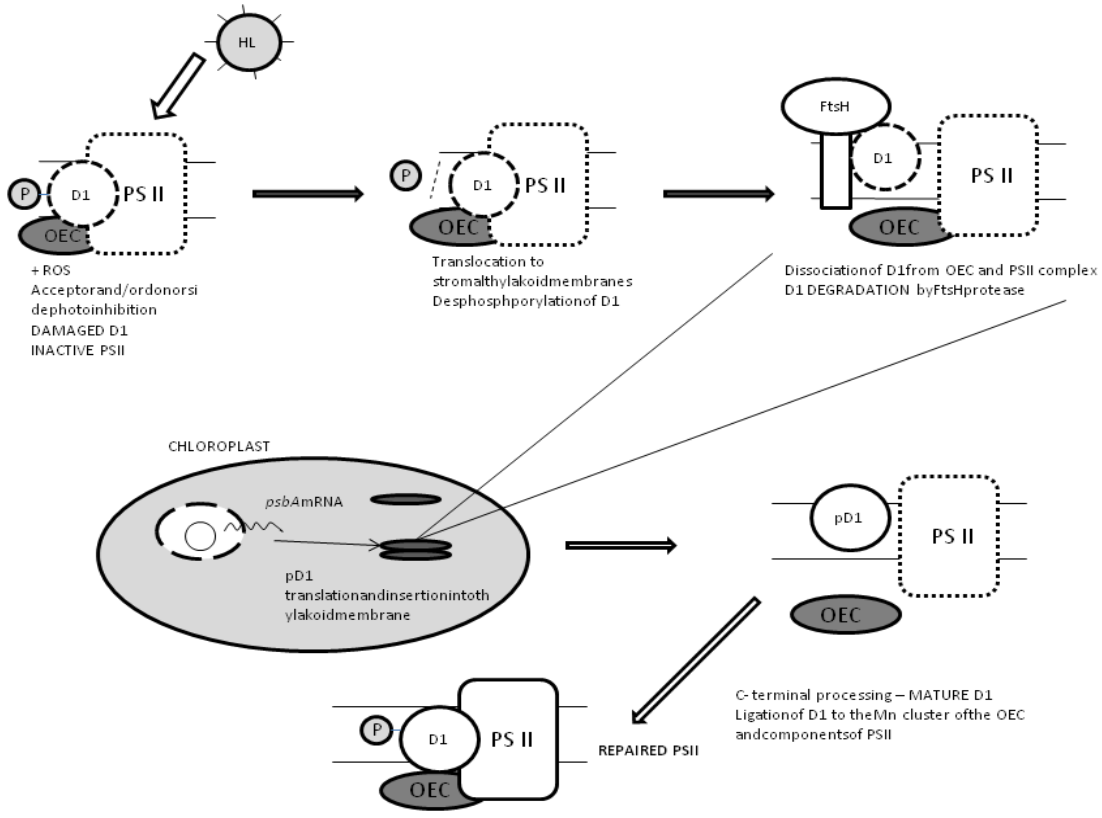

Figure 3 – A model for D1 repair. D1 is highlighted from the PSII complex for illustrational purposes. During photodamage, small CAB-like proteins (SCPs, or HLIPS) protect the

complex, probably avoiding dephosphorylation of the different components, including D1, until it arrives at the site of repair in the stroma thylakoids. There, proteolysis of damaged D1 protein in the thylakoid membranes is conducted by a FtsH2/3 protease complex after CP43 (not depicted) is separated from the rest of the complex and possibly a deg protease also has some role in degradation. A new D1 copy is brought to the site of repair and is inserted into PSII. Adapted from Nixon et al. (2010).

Several FtsH proteases in the stroma side thylakoid membranes are proven to be strictly necessary for D1 degradation (Yoshioka and Yamamoto, 2011). From the Htr/Deg family, HtrA and DegP proteases can also cleave D1, although they are not considered required (Silva et al., 2003). Owing to the diverse and contradictory information it seems plausible to consider that Deg1, 2 and possible other proteases cleave hydrophilic regions of D1 and then FtsH degrades the fragments (Edelman and Mattoo, 2008; Yoshioka and Yamamoto, 2011). Various cleavage sites have been detected and this has suggested a role of D1 fragments in controlling stressful events and even repair (Edelman and Mattoo, 2008).The nature of the signal, which proteases are responsible for D1 proteolysis in each situation and the idea that D1 can actually have a role in controlling repair, are issues that still need more investigation. First experiments indicated a role of phosphorylation in D1 degradation, as pointed by Elich et al. (1992) and Kettunen et al. (1991), as it was discovered that D1 is phosphorylated before insertion into membranes, that light affects the rate of phosphorylated D1, and that dephosphorylated D1 becomes a substrate for proteolysis. These authors hypothesized that this would act as the signal for degradation. Nowadays it is seen more as a mechanism to prevent PSII from collapsing before migration of the whole complexes to the sites of repair, but dephosporylation must occur for D1 degradation to happen (Aro et al., 2005). Since then, much research has focused on repair mechanisms, and it doesn't seem that D1 degradation is necessarily tied that tightly to photoinhibition (Edelman and Mattoo, 2008). To assess quantum yield of photosystem II for studying photosynthetic activity, a common method employed is pulse-amplitude modulated fluorescence.

Fluorescence as a measure of photosynthetic activity and stress effects

The process of light absorbance by pigments provides a way for photosynthesis to be measured. Chlorophylls or other pigments absorb light and transmit it to the reaction centres. Mainly chlorophyll *a* exists in the antennae, but as mentioned before, this can vary with species. If too much light acts on pigments, there might not be enough reaction centres open to capture all the excitons provided, and so more energy must be dissipated as heat or fluorescence (Falkowski and Raven, 1997). In 1931, Kautsky discovered that upon illumination of a dark-adapted leaf there was a rapid rise in fluorescence, followed by a slow decline - the Kautsky effect (Govindjee, 1995). Reaction centres are said to be open if they are able to use the energy of an absorbed photon to transfer an electron to plastoquinone (abbreviated Q from fluorescence 'quencher'). When plastoquinone is reduced, photons arriving at the reaction centre cannot be used until the next acceptor has received the electron, reoxidizing plastoquinone. The reaction centre is said to be closed in this situation. When reaction centres are closed, more photons are reemitted as fluorescence. All reaction centres are open when cells are dark-adapted. In pulse-amplitude modulated (PAM) fluorometry a saturating pulse of light is used to close all reaction centres rapidly, and F_m, the maximum fluorescence, is obtained. F_0 is the minimum constant fluorescence in the dark when all reaction centres are open (Ruban and Johnson, 2010) and variable fluorescence, F_v, is the fluorescence value that results from the subtraction of F_0 from F_m (Kooten and Snel, 1990). The maximum value of fluorescence of dark-adapted chloroplasts subjected to a saturating light pulse is used as the maximum fluorescence that can be achieved. If the photosynthetic apparatus is subjected to a given actinic intensity of light, the basal fluorescence is denoted as F_0' (minimum fluorescence of a photosynthetic apparatus adapted to a given actinic light intensity), and a saturating pulse at the same actinic light intensity determines F_m', the maximum fluorescence at the given light-adapted conditions (Cartaxana and Serôdio, 2008), changing consequently F_v. The maximum potential quantum yield of photosystem II is given by the ratio F_v/F_m, measured in dark-adapted material. In light-adapted samples, the effective quantum yield of PSII is given by the product of the quantum yield of light-adapted PSII reaction centres by the photochemical quenching coefficient, qP, which represents the fraction of open PSII reaction centres. Rapid-light curves (RLCs) further provide estimation of photosynthetic efficiency (α), the capacity, given by the maximum relative electron transport rates (ETR_m) and the light-saturation index (E*k*) (Belshe et al., 2007; Serôdio et al., 2006; White and Critchley, 1999), by building curves that relate PAR intensity and the observed

ETR, and the later with the expected ETR (Platt and Jassby, 1976). As such, yields can be used to estimate the photosynthetic activity of chloroplasts at any given light intensity, and in different stressful conditions if wished.

Phaeodactylum tricornutum as a model to study D1 and photoprotection

P. tricornutum is one of the most extensively studied phytoplanktonic species for molecular physiological processes, and there is some data available for D1 dynamics during stressful events, mainly high light, that try to explain the repair processes of photosystem II (Wu et al., 2011). In fact, there are several laboratory strains and even natural strains which exhibit diverse behaviour and different patterns of protection to stress, such as varied PSII yields, NPQ rates, or even in the time of the response and the way it happens (Lavaud et al., 2007). This, in itself, reveals the tremendous adaptations that occur even intraspecifically among phytoplankton, which appears to be more evident in diatoms. *P. tricornutum* has been shown to be a particularly resistant species to photodamage (Lavaud et al., 2007; Nymark et al., 2009), having high NPQ capacities and efficient and quick repair mechanisms when subjected to high light (Lavaud et al., 2002). Studies using mutants for D1 protein (Materna et al., 2009), also in other species, reveal the importance of the C-terminal extension of the precursor protein, which is still open for debate, or the dynamics of repair mechanisms and degradation by the identified proteases FtsH and Htr/Deg, and the different cleavage sites in D1. For this reason, it is suspected that D1 fragments originated may actually have a role in controlling repair or other acclimation to light processes, as light highly controls D1 degradation and resynthesis (Nixon et al., 2010). In *P. tricornutum* there is a highly coordinated change in the usual constitutive and photoprotective pigments in response to high light. Even in prolonged high irradiances they are able to dissipate excessive light energy rather efficiently, which confers them photosynthetic and photoprotective flexibility under constant changing light intensities (Lavaud et al., 2002). D1 profiles during these acclimation phases are still missing though, and it has been shown that there is such a complex mechanism that a simple approach is probably not suitable. However it can provide an idea of what is happening when crossed with other data, to elucidate at which time of the repair important variations are happening, as to focus on them in the future and address the problem in a more specific manner.

Objectives

The main objective of the present thesis is to search for photoinhibition effects on the D1 protein after 1 h of low light (40 µmol.m^{-2}.s^{-1}) and high light stress at 1,250 µmol.m^{-2}.s^{-1}, using the model diatom species *P. tricornutum*. Furthermore, the capacity of recovery of D1 is also of interest, thus the comparison of control samples at different light intensities with chloroplast-protein synthesis inhibited samples. It is also intended to relate effects of D1 content with quantum yield of photosystem II at the same conditions as to provide information on the effects of D1 degradation on electron transport along the photosynthetic chain. Finally, the energy dissipation mechanism of NPQ and pigment concentrations will be determined to infer on photoacclimation of this diatom. A major part of the present work was the optimization procedure of an efficient protocol for D1 protein extraction, immunodetection and absolute quantification.

Cultures and samples

Monoalgal cultures of *Phaeodactylum tricornutum* IO 108-01 (Fig. 4A), isolated from samples from Ria de Aveiro (Aveiro, Portugal)were grown in f/2 medium in a growth chamber (Fitoclima 250E, Aralab, Fig. 4B)at 15ºC and 40 µmol.m^{-2}.s^{-1} irradiance (12:12 h photoperiod). Cultures used for the experiment were grown in flasks and sampled at exponential phase. Low light (LL) cultures were maintained at the same growing conditions specified above, while high light (HL) stress cultures were transferred to a Fytoscope FS130 (Photon Systems Instruments) for 1 h at 1,250 µmol.m^{-2}.s^{-1} and 15ºC.Half of the samples from each treatment were inoculated with lincomycin at 0.4 mg/mL (LLi and HLi), an inhibitor of chloroplast-encoded proteins, including D1. The inhibitor was added to the cultures 30 min before light stress. Four replicates were used for each treatment.

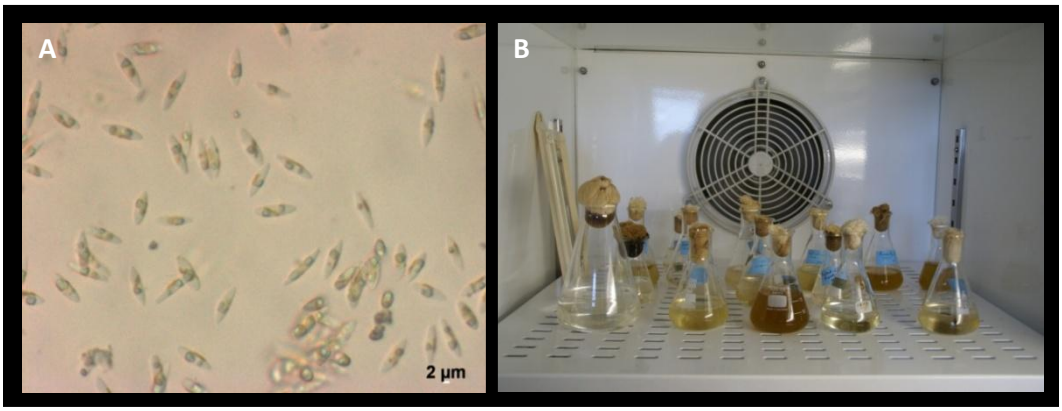

Figure 4 – A) *Phaeodactylum tricornutum* IO 108-01 as seen in an inverted microscope Olympus IX70 (Olympus Corporation, Tokyo, Japan), 100 x; and B) Cultures in the growth chamber (Fitoclima 250E, Aralab, Portugal).

Protein extraction

Culture samples (20 mL) were rapidly filtered through 0.45 µm pore GF/F Whatman filters and immediately immersed in liquid nitrogen. Microalgae were scratched off the filters

using a spatula to an eppendorf containing 1 mL of extraction buffer. 500 mL of this buffer were prepared previously [10.125 mL Na_2HPO_4 0.2 M; 2.375 mL NaH_2PO_4 0.2 M; 2.5 mL EDTA 0.1M; 0.2% Tween 20, or polyethylene glycol sorbitan monolaurate) (v/v) and 231 mL Milli-Q H_2O). 10 µL PMSF (phenylmethylsulfonyl fluoride) 1mM and 4 µL dithiothreytol (DTT) 2 mM were then added directly to eppendorf tubes at the time of extraction. Tubes were vortexed until the contents were completely homogenized. Samples were frozen in liquid nitrogen until extraction began. Samples were then put in a 5 min bath (Polystat 86602, Thermo Fisher Scientific, Waltham, USA), at 80ºC, sonicated (Bransonic 220 V, Danbury, USA) for 1 min and gently mixed. The freeze-thaw cycle was repeated 4 times. To remove the disrupted cells, samples were centrifuged at 10,000 g for 20 min at 4 ºC and the supernatants with the proteins were collected. The efficiency of the extraction method was estimated by 2 additional extractions of the remaining pellets, until residual or null amount of protein was detected in the extracts. Protein concentration was determined with Bradford microassay using bovine serum albumin (BSA) as protein standard, using known concentrations of this protein. The obtained equation, plotting BSA concentration vs. Abs_{595} nm, was used to quantify the total amount of protein in each extract. For a total volume of 1 mL, 50 µL of extract were mixed with 750 µL of Milli-Q water and finally 200 µL of concentrated Bradford reagent. Tubes were gently mixed to avoid foaming, and after 15 minutes they were transferred to cuvettes and absorbance at 595 nm was read in a Unicam UV500 spectrophotometer (Thermo Fisher Scientific, Waltham, USA).Samples were stored at -80ºC.

Western immunoblotting of the D1 protein

Proteins were separated by SDS-PAGE using a mini-gel system from Bio-Rad (Hercules, USA, Fig. 5A). 2 µg of extracted total protein, diluted in12 µL extraction buffer and 4 µL of sample buffer (4x), were loaded into each well and were allowed to separate for 60 minutes at 150 V. Protein standards (Novex from Invitrogen, Carlsbad, USA) were used to know protein size and control migration. Protein transfer to nitrocellulose membrane from gels was done in a Semi-Dry transfer tank from Bio-Rad (Fig. 5B), using extra thick blot paper and immersing it and the membrane in transfer buffer (10 mL Tris-HCl pH8 1M; 5.76 g glycine; 80 mL methanol; H_2O Milli-Q to 400 mL). The membrane was allowed to be

immersed for at last 10 minutes in transfer buffer. The blot paper was then put on top of the metal plate, followed by the membrane, then the gels on top, and finally more blot paper. Bubbles were removed by pressing the assemblage with a rolling instrument and the extra buffer that spreads on the plate was removed. The transfer was allowed to go on for 1 hour at constant 140 mA and 20 V. Membranes were taken off and washed in Phosphate buffer saline with Tween 20 (PBS-T 1x) [prepared from PBS-T 10x (80 g NaCl; 2 g KCl; 14,4 g Na_2HPO_4; 2,4 g KH_2PO_4; 20 mL Tween 20; H_2O Milli-Q to 1 L; pH 7.4)] for 15 min. To verify if Bradford quantification was successful and equal amount of protein was loaded into the SDS-PAGE wells and transferred to the membrane, Ponceau dye [0.1% (w/v) Ponceau S in 5% acetic acid] was allowed to contact the membrane for 15 s, then the membrane was rinsed with water until red bands were seen. For further confirmation of transfer, gels were stained overnight with Coomassie blue coloration medium (1 g Coomassie blue; 200 mL methanol; 100 mL acetic acid; H_2O to 1 L) and washed the next day with discoloration medium (250 mL ethanol; 100 mL acetic acid; H_2O to 1L). Membranes were blocked with Amersham ECL Advance kit's blocking reagent (GE Healthcare, Buckinghamshire, United Kingdom) or dry milk (5%) diluted in PBS-T buffer, being agitated for 1 h at room temperature. Rabbit anti-psbA antibody from Agrisera (Vännäs, Sweden) was used for detection of D1, being incubated in the buffer-powder mix at 1:20,000 dilution for 1 h. The membrane was then washed 4 times for 15 min in PBS-T buffer and finally the secondary IgG anti-rabbit antibody conjugated with horseradish peroxidase (GE Healthcare) was incubated for 1 hour (1:40000). A final wash step was done 4 times for 15 min in PBS-T (Fig. 5C). In the dark chamber, the membrane was put for 5 min in a mixture of solution A and B from the ECL Advance kit, at 1:1 proportion. The membrane was put into a hypercassete (GE Healthcare) and the film was allowed to contact it for 1 s. The film was then revealed and finally fixed. Films were imaged with a Versadoc white light conversion plate in a Gel Doc XR imaging system (Fig. 5D) to quantify band intensities by densitometry, using Quantity-One software (all Bio-Rad). psbA/D1 protein standard (Agrisera) was used in the blots, in order to have a known amount of protein to compare the extracts with, and determine protein concentrations in pmol by using 3 known concentrations of D1 (0.025; 0.15 and 0.3 pmol). A linear relation was obtained measuring chemoluminescence from the Protein Standard with Quantity One. The acquired equation was used to determine the concentration of D1 in the extracts.

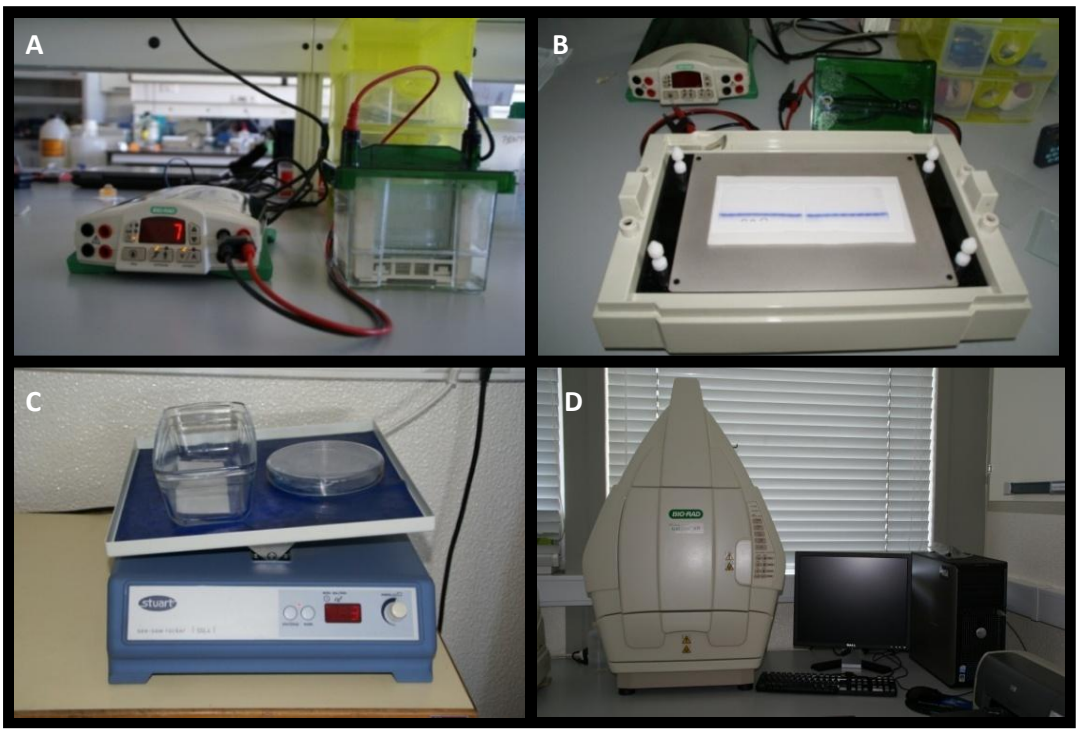

Figure 5 – Protein blotting steps after extraction and Bradford quantification. SDS-PAGE (A), transfer to nitrocellulose membrane (B), incubations with antibodies and washing steps (C) and molecular imager system used for densitometry (D).

PAM fluorometry

Monoalgal cultures of *Phaeodactylum tricornutum* (1.2 mL) were used, with and without lincomycin. Samples were transferred to a Clark-type liquid-phase oxygen electrode chamber (DW2/2 electrode chamber, Hansatech Instruments Ltd., Norfolk, UK) and kept homogeneous by constant mixing. Temperature was maintained at 15ºC by a circulating water bath (Haake K10/C10, Thermo Scientific, USA). All fluorescence measurements were performed using a PAM 101 fluorometer (Walz GmbH, Effeltrich, Germany, Fig. 6) connected to a PAM Data Acquisition System PDA 100 (Walz, Effeltrich, Germany) controlled by the software WinControl v2.08. External light sources were used to provide actinic light (KL 1500 LCD Schott AG, Mainz, Germany) and the saturating light pulses (KL 2500 LCD, Schott AG,Mainz, Germany). F_V/F_m = $(F_m - F_0)/F_m$ was determined as the maximum yield of dark-adapted samples, 10 min after being put in the dark (Kitajima and Butler, 1975). Afterwards a Rapid Light Curve (RLC) was obtained using 8 different light intensities (31, 48, 93, 167, 278, 560, 820 and 1007 µmol photons.m^{-2}.s^{-1}), applying saturating

pulses after periods of 30 s each. The product of F_v'/F_m' times qP was computed as the effective quantum yield of photosystem II in light (Genty et al., 1989). Non-photochemical quenching (NPQ) was determined as $(F_m-F_m')/F_m'$ (Bilger and Bjorkman, 1994). The samples were the illuminated for 1 h with 1,250 µmol photons.m^{-2}.s^{-1} PAR. Quantum yield was measured immediately before the end of the light stress period and during the recovery in the dark: light pulses were applied at 2, 5, 8, 13, 20, 30 and 60 min in dark. After a 24 h period in the dark at 15ºC, the yield was again measured for determination of total recovery and another RLC was performed. The model of Platt and Jassby (1976) was adjusted to the RLCs and the initial slope of the light curve (α), the photoinhibition parameter (β), the maximum relative ETR ($rETR_m$) and the light saturation parameter (E*k*) were computed.

Figure 6 – The PAM 101 fluorometer (a) connects the data acquisition system (b) the light sources (f) and the computer. Samples are put into the DW2/2 electrode chamber (Hansatech Instruments Ltd., Norfolk, UK) (c), fixed onto a magnetic mixer (d). A *Haake* K10 bath system (Thermo Fisher Scientific, Waltham, USA) (e) is used to keep the chamber at 15ºC with circulating water.

Pigment analysis by HPLC

10 mL from each of 4 replicates of the 4 different treatments were rapidly filtered using 25 mm GF/F (Whatman) filters and immediately frozen in liquid nitrogen. Pigment extraction was performed by homogenizing the filters in 95% cold buffered methanol (2% ammonium acetate) using a rod. Samples were then sonicated for 30 s, briefly mixed and transferred to -20ºC for 30 min. Supernatants were collected after centrifugation for 5 min at 4,000 rpm and 4ºC, being filtrated through 0.2 µm Millipore membrane filters. Extracts were injected into a Shimadzu HPLC system (Kyoto, Japan, Fig. 7) with a photodiode array detector (SPD-M10AVP). Chromatographic separation was carried out using a C18 column for reverse phase chromatography (Supelcosil; 25 cm long; 4.6 mm in diameter; 5 µm particles) and a 35 min elution programme. Flow rate applied was of 0.6 $mL.min^{-1}$. Identification and calibration of the HPLC peaks was done using pigment standards from DHI (HØrsolm, Denmark). Pigments were identified from absorbance spectra and retention times and their concentrations were obtained from the signals in the photodiode array detector.

Figure 7 – Extracts are put into the auto-sampler (a), which injects automatically the samples into the HPLC system, maintained at 1ºC by a cooler (b) which are sent into the chromatographer (c). Solvents (d) are sent through the degasser (e) to the chromatographer (c). From here samples diluted in solvents go through the separation C18 column (f) where they bind and come out at different times. As the different pigments leave the column absorbance is read by the photodiode array detector (g) and chlorophyll fluorescence is

obtained by the fluorescence detector (h). The system is controlled by i (system controller SCL-10A) and data is visualized and analyzed with software Class-VP (j).

Data and statistical analysis

Data was treated with *Quantity-One* (Bio-Rad), *Excel* (Microsoft Office 2007, Seattle, USA) and *SigmaPlot 11* (Systat Software, Chicago, USA), which were also used for statistical analysis. Descriptive statistics were conducted mainly in *Excel*. Data was then transferred to *SigmaPlot 11* where significant differences among treatments for all experiments were searched for. Linear regressions were used for Bradford microassay calibration curves (*Excel*) and for obtaining D1 concentrations in samples from known ones from purified D1 (*Quantity-One*). For determination of differences in D1 content with low and high light treatments, each with or without protein synthesis inhibitor, two-way analysis of variance (ANOVA) was used. For pigment content the same analysis allowed to search for significant differences on contents of the different de-epoxidation states of xanthophylls (diadinoxanthin and diatoxanthin), other major pigments such as fucoxanthin, chlorophylls *a*,*c*2 and β-carotene and pigment ratios such as DT/(DD+DT), DD/(DD+DT) and (DD+DT)/Chl *a*. For PAM fluorometry also two-way ANOVA was used to determine differences in quantum yields, NPQ and RLC parameters α, β, $rETR_m$ and E*k*. Kruskal-Wallis. One-way ANOVA on Ranks was used to determine the effect of the presence or absence of inhibitor on recovery of quantum yield of photosystem II, in samples subjected to high light. The effects of the inhibitor on different light intensities before and after high light stress induction were accounted for. Significance levels were set to 95% (α=0.05).

Protein extraction

Extraction from both soluble and membrane-bound proteins from *P. tricornutum* required optimization. Several procedures were employed until the best results were obtained. After trying several modifications such as homogenization in liquid nitrogen or more sonication cycles, a procedure resulting in 98.2 ± 1.06 % efficiency was obtained (Table I).

Table I – Efficiency of protein extraction to *P. tricornutum* (total protein content of 1st extraction/ total protein extracted in all three extractions, n=8):

Extraction	Total protein extracted (µg/mL extract)			Efficiency (%)
	1st	2nd	3rd	
Replicates	273	2,95	0,90	98,6
	305	1,53	7,85	97,0
	307	1,83	*	99,4
	248	3,78	5,42	96,4
	303	1,74	4,65	97,9
	285	2,13	*	99,3
	280	1,63	1,81	98,8
	217	1,35	3,38	97,9
Average				**98,16**
s.d.				**1,06**

* No protein detected

Optimization of the assay involved finding the right Bradford test to be employed. The standard assay is used for higher concentrations of protein (>25 µg protein/mL), while the microassay is used for concentration of 1-20 µg/mL. This mL refers to the volume in the cuvette during quantification with Bradford reagent. The number of cells of *P. tricornutum* grinded provided only a small amount of protein. For this reason, the microassay was employed using 50 µL of extract. Bradford assays require a calibration curve (Fig. 8) based on the absorbance values at 595 nm given by the reaction of a known protein (BSA being the most commonly used) with the Bradford reagent. Each new set of measurements requires a new calibration to be performed.

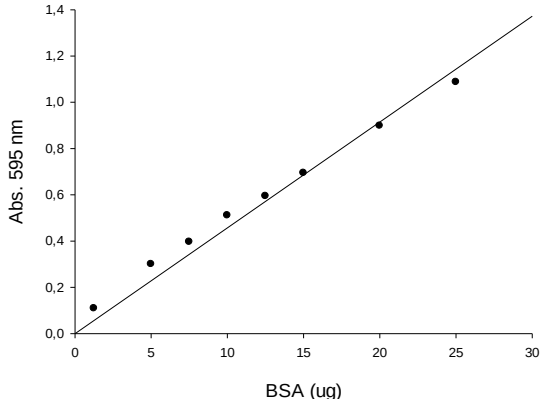

Figure 8 – Bradford microassay calibration curve with BSA. Linear regression, y = 0,0405x + 0,0859; r^2 = 0,998.

Table II - Bradford microassay quantification of *P. tricornutum* protein extracts in the four treatments tested (n=4). Protein concentration was calculated using the equation y = 0,037x + 0,0575; r^2 = 0,992. LL (low light, 40 µmol photons.m^{-2}.s^{-1}); HL (high light, 1,250 µmol photons.m^{-2}.s^{-1}); LLi (low light with lincomycin); and HLi (high light with lincomycin). 1,2,3 and 4 are replicates for each treatment:

Amount of total protein extracted					
	Abs. 595 nm				Total protein
	a)	b)	c)	Average	extracted (µg/mL)
LL1	*	0.637	0.639	0.638	**273**
LL2	0.773	0.761	0.74	0.758	**332**
LL3	0.758	*	0.753	0.756	**331**
LL4	0.774	0.765	0.782	0.774	**340**
HL1	0.667	*	0.68	0.674	**290**
HL2	0.704	*	0.702	0.703	**305**
HL3	0.707	*	0.71	0.709	**307**
HL4	0.581	0.594	*	0.588	**248**
LLi1	0.704	*	0.693	0.699	**303**
LLi2	0.615	*	0.616	0.616	**262**
LLi3	0.730	0.710	0.712	0.717	**312**
LLi4	0.849	0.847	0.851	0.849	**377**
HLi1	0.678	0.680	*	0.679	**293**
HLi2	0.663	0.662	*	0.663	**285**
HLi3	0.653	0.662	0.642	0.652	**280**
HLi4	0.527	*	0.523	0.525	**217**

* Discrepant readings.

The equation obtained in Fig. 8 was used to determine the amount of protein in a determined volume (50 µL) of the extracts, and then total amount of protein in the whole volume of extract (1 mL) is calculated. Three replicates of each extract were measured, and their average value of absorbance was used to obtain the mass of total protein extracted in 1 mL of extraction buffer (Table II).

Finally, knowing the amounts of protein in each extract, the required volume of each was used for the western blot analysis, in order to have 2 µg of protein. The quantity of protein to be used was suggested by the antibody manufacturer (Agrisera).

D1 detection and quantification

The volume of each extract of the 4 treatments corresponding to 2 µg of protein was put into sample buffer for SDS-PAGE separation by protein size. Optimization of the western blot followed the indications the psbA/D1 antibody manufacturer provided, although 1 µg of protein showed to be sufficient (data not shown). Transfer to membrane was done firstly onto small membranes, and thus the transfer time was shorter (30 min). For the larger membranes, necessary to quantify all samples at the same time, 60 min were used. Fig. 9 shows the result of the first of two identical experiments (abbreviated Exp in figures), using the same number of replicates and the same treatments. The results, as will be shown, were similar.

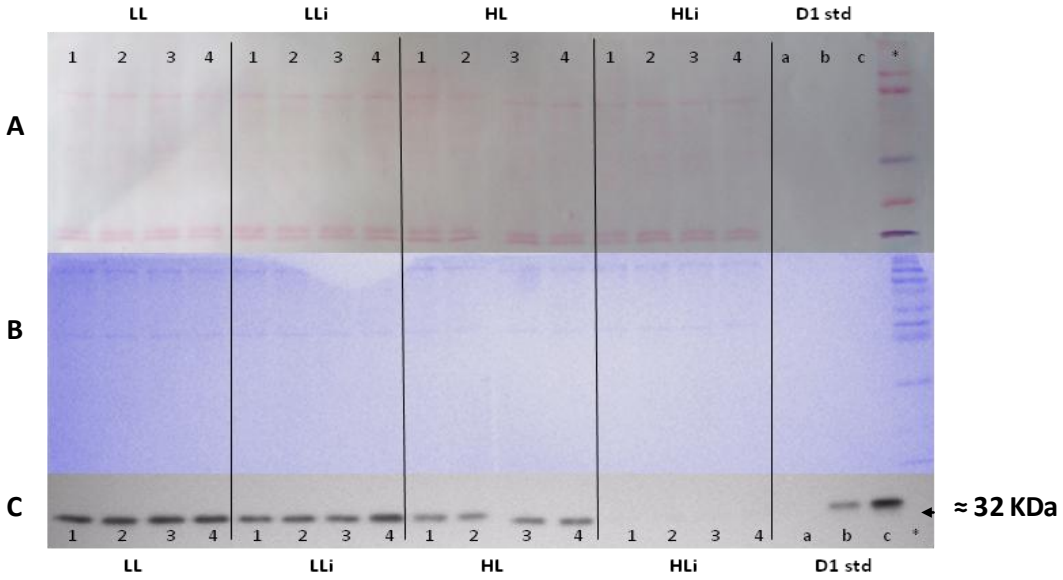

Figure 9 – Western blotting (experiment 1) of D1 protein from *P. tricornutum* in the four treatments: LL (low light, 40 µmol photons.m^{-2}.s^{-1}); HL (high light, 1,250 µmol photons.m^{-2}.s^{-1}); LLi (low light with lincomycin); and HLi (high light with lincomycin). 1, 2, 3 and 4 are replicates for each treatment. D1 std a, b and c are D1 standards at 0.025, 0.15 and 0.3 pmol, respectively; and * isthe protein ladder. A is the membrane dyed with Ponceau, B is the gel coloured with coomassie blue and C is the film after chemoluminescent treatment to membranes.

After transfer, to ensure proteins were successfully transferred to the nitrocellulose membranes, these were dyed with Ponceau reagent, which is red and binds to proteins (Fig. 9A). As it is seen, transfer occurred and most importantly, the same amount of total protein was loaded into each well of the polyacrylamide gels, revealing correct quantification with the Bradford assay and assuring that D1 detection and differences in intensities of bands can be indicative of different amounts of D1 per treatment. To confirm that proteins were transferred the remaining gels were dyed with Coomassie blue coloration medium (Fig.9B). In dyed gels prior to transfer, proteins were much more abundant, and while some bands are seen, these correspond to the higher molecular weight proteins, which don't transfer as quickly onto the membrane and thus remain in the acrylamide gels, unless they are given more time to transfer.

Fig.9C shows the final western blot results, where bands shown correspond to chemoluminescence resulting from the reaction of the added substrate from the ECL advance kit with the enzyme conjugated to the secondary antibody, after incubations with primary (anti-psbA) and secondary antibodies.

The imaging software (*Quantity-One*) calculates various parameters, such as the adjusted volume, which corresponds to the intensity of the band in arbitrary units (arbitrary units of intensity*mm^2, a.u.) in a specific area, and subtracts the intensity of the background. This value was used to obtain the relative quantity of D1 in the different treatments (Fig. 10). Based on band densities, as it is shown in Figs. 9, 10 and 11, a D1 decrease occurs in all treatments in relation to low light control treatment.

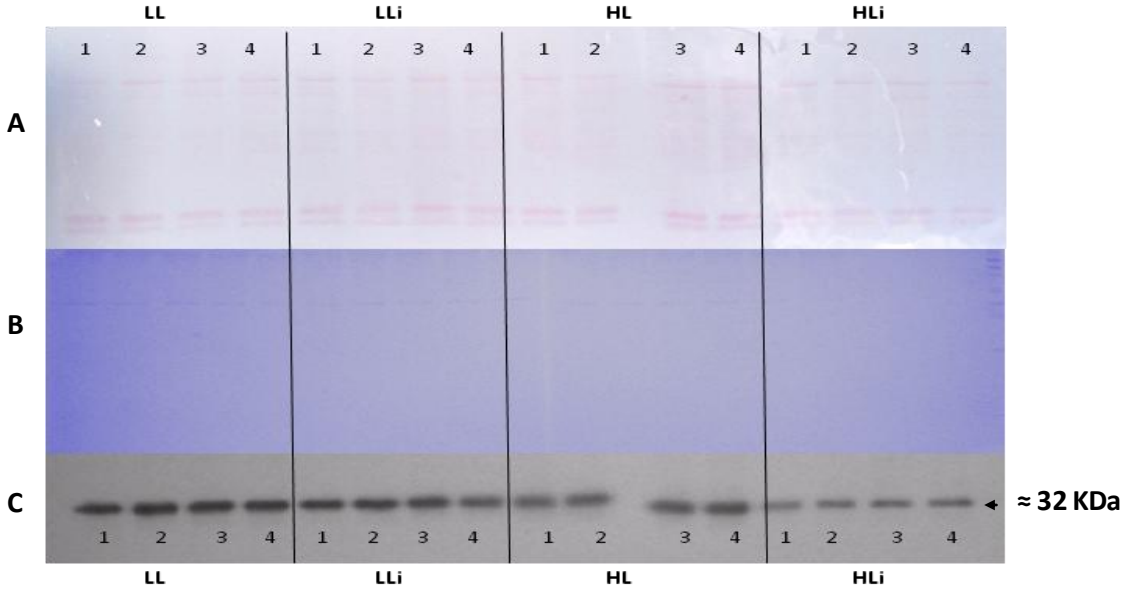

Figure 10 – Western blotting (experiment 2) of D1 protein from *P. tricornutum* in the four treatments: LL (low light, 40 µmol photons.m^{-2}.s^{-1}); HL (high light, 1,250 µmol photons.m^{-2}.s^{-1}); LLi (low light with lincomycin); and HLi (high light with lincomycin). 1, 2, 3 and 4 are replicates for each treatment. A is the membrane dyed with Ponceau, B is the gel coloured with coomassie blue and C is the film after chemoluminescent treatment to membranes.

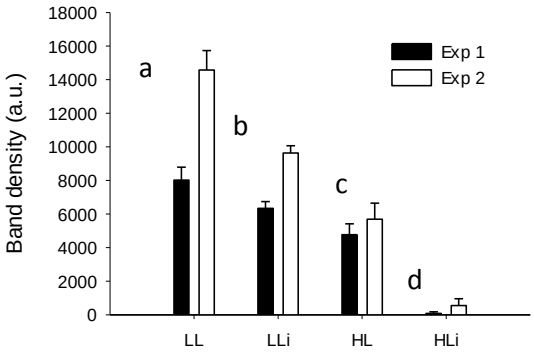

Figure 11 –Western blotting densitometry of D1 protein [(INT*mm^2)-Background] from *P. tricornutum* in both experiments in the four treatments: LL (low light, 40 µmol photons.m^{-2}.s^{-1}); HL (high light, 1,250 µmol photons.m^{-2}.s^{-1}); LLi (low light with lincomycin); and HLi (high light with lincomycin).

The data acquired for experiment 2 reveals the same pattern in D1 content among the treatments than experiment 1. Once again, Fig. 10A represents coloured nitrocellulose membrane with Ponceau dye, Fig. 10B the stained gels after transfer and Fig. 10C the film with the final western blotting results. The shown film results correspond to a prior run where 4 replicates for each treatment were loaded and no D1 standard was used. Quantification was done using only three replicates for experiment 2 (not shown), where standard D1 protein was used. *Quantity-One* allows the construction of calibration curves, by corresponding a known amount of the protein that was loaded into each well to each band intensity. The best relation obtained is then used to obtain the equation that will allow for D1 quantification in fmol. A good linear relation was possible for both experiments (Fig. 12 and 13).

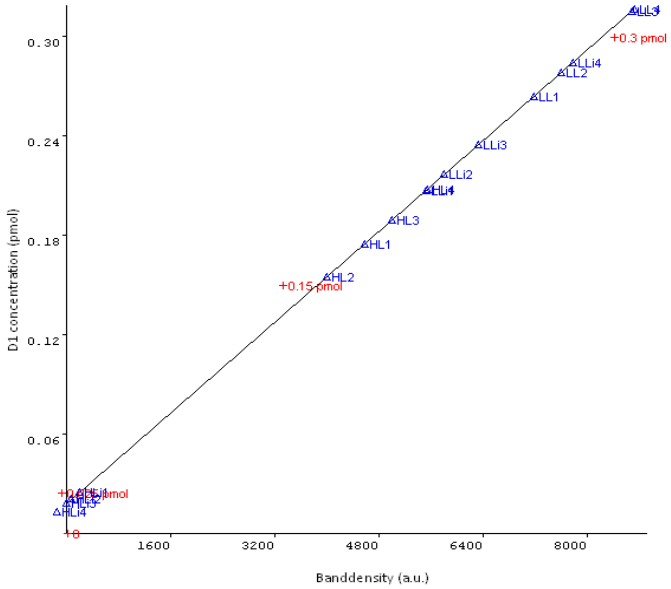

Figure 12 – Linear adjustment ($3.44x10^{-5}$.Vol + 0.0183; r^2 = 0.99) using standard D1 protein (Agrisera) densitometry of D1 protein [(INT*mm^2)-Background] from *P. tricornutum* in experiment 1 in the four treatments: LL (low light, 40 µmol photons.m^{-2}.s^{-1}); HL (high light, 1,250 µmol photons.m^{-2}.s^{-1}); LLi (low light with lincomycin); and HLi (high light with lincomycin). Blue triangles are replicates of the various treatments and red crosses are standard concentrations of D1 (n=4).

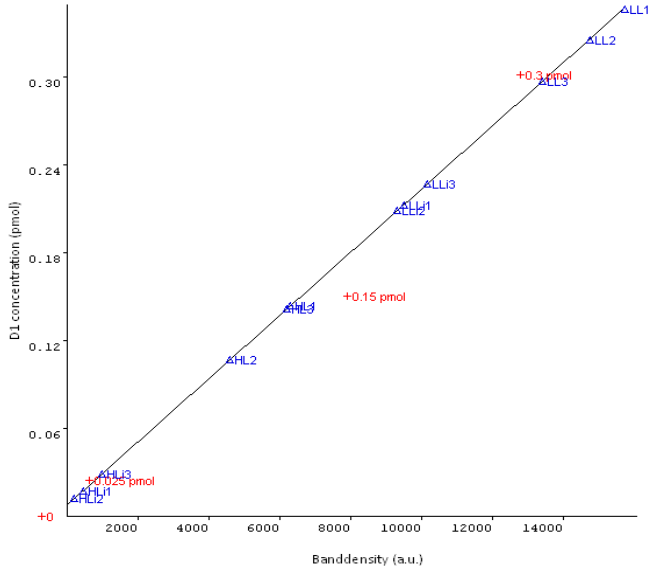

Figure 13 – Linear adjustment ($2.15x10^{-5}$.Vol + 0.00812; r^2 = 0.98) using standard D1 protein (Agrisera) densitometry of D1 protein [(INT*mm^2)-background] from *P. tricornutum* in experiment 2 in the four treatments: LL (low light, 40 µmol photons.m^{-2}.s^{-1}); HL (high light, 1,250 µmol photons.m^{-2}.s^{-1}); LLi (low light with lincomycin); and HLi (high light with

lincomycin). Blue triangles are replicates of the various treatments and red crosses are standard concentrations of D1. Quantification was done on another gel run after the one shown in Fig. 10, where standard D1 was added. Here only 3 replicates were used (n=3).

Using the linear regression equation obtained with band intensities from D1 standards concentrations, D1 concentrations from all replicates were calculated in fmol expressed by 1 µg of total protein extracted (Fig. 14).

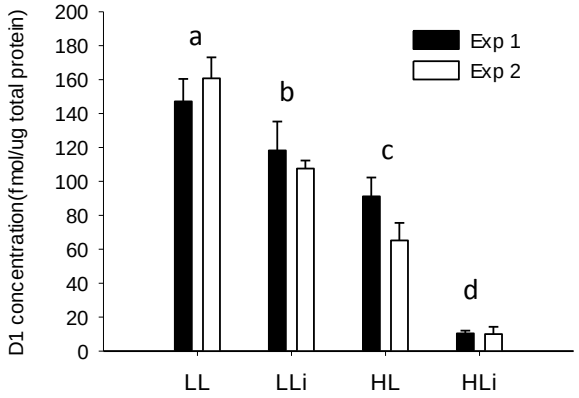

Figure 14 – Quantification of D1 protein with *Quantity One* (Bio-Rad) in fmol in experiment 1 and 2 (n= 4 and 3, respectively). Purified D1 protein standard (Agrisera) was used for calibration, and a linear adjustment was used to calculate D1 content in each sample. D1 protein content is shown in fmol/µg of total protein from *P. tricornutum* in all 4 treatments tested: LL (low light, 40 µmol photons.m^{-2}.s^{-1}) and HL (high light, 1,250 µmol photons.m^{-2}.s^{-1}) and same 2 but with chloroplast protein synthesis inhibitor lincomycin (i).

For experiment 1, Fig. 14 shows a decrease in high light treatment (91 fmol/µg total protein), particularly evident when chloroplast encoded protein synthesis is inhibited with lincomycin (11 fmol/µg total protein). Even in low light, degradation of D1 occurs, although it is only a slight decrease from the non-inhibited to the inhibited treatment, from 147 fmol to 118 fmol/µg total protein in experiment 1. In experiment 2 LL treatments, a descrease from non-inhibited to inhibited cultures occurs, from 160 to 107 fmol/µg total protein. In HL its decrease is to 65 fmol/µg total protein and when inhibitor is added it goes down to 10 fmol/µg total protein. Translating the 1st experiment results into D1 degradation [(D1 in LL – D1 in LLi) / D1 LL and [(D1 in HL – D1 in HLi) / D1 HL] expressed as percentage of control (LL),

in high light more than 38% of the D1 protein pool disappears, and inhibiting protein resynthesis provokes a 93% decrease in D1 content. All treatments behaved differently in these experiment ($P<0.001$), as shown with two-way ANOVA with Tukey test for groups comparison, meaning there is an effect of the inhibitor in each light treatment for both density, D1 content in fmol/µg total protein and % of D1 degraded based on LL controls. Treating in the same way the 2nd experiment shows a 33% decrease in LLi, 59% in HL and 94% in HLi.

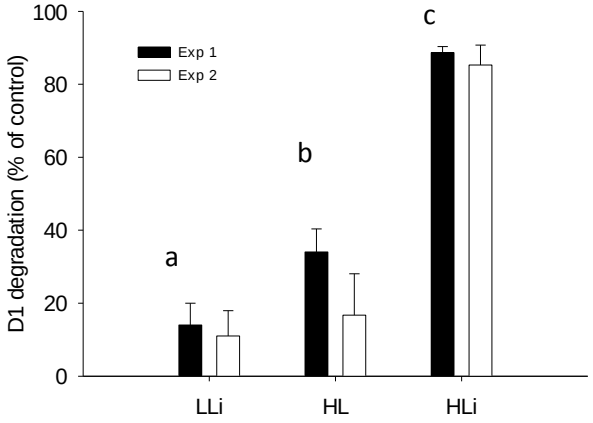

Figure 15 – D1 degradation in *P. tricornutum* in the four treatments, expressed as % of LL (low light, 40 µmol photons.m^{-2}.s^{-1}): HL (high light, 1,250 µmol photons.m^{-2}.s^{-1}); LLi (low light with lincomycin); and HLi (high light with lincomycin). Percentages calculated from fmol/µg total protein values.

The pattern of D1 degradation is similar in both separate experiments, being clear that D1 degradation occurs at all light intensities, but being much more evident in high light intensities. The inhibited treatments provide a way for estimation of D1 repair and turnover (Fig. 16).

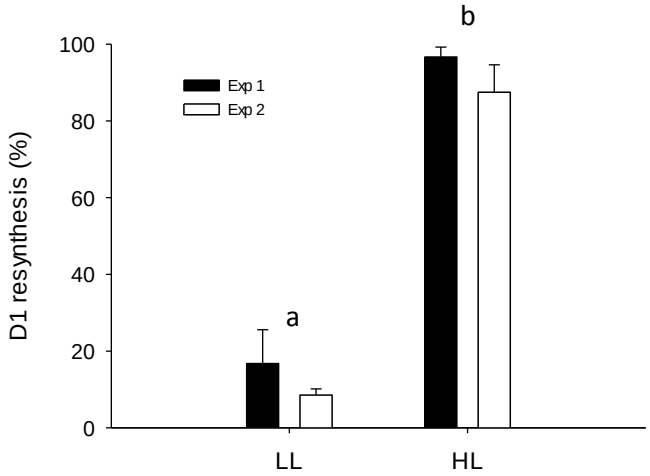

Figure 16 – D1 protein resynthesis in *P. tricornutum* at LL (low light, 40 µmol photons.m^{-2}.s^{-1}) and HL (high light, 1,250 µmol photons.m^{-2}.s^{-1}). Resynthesis (%) was calculated as (D1 concentration at LL – D1 concentration at LLi) / D1 concentration at LL, and same for HL, (D1 concentration at HL – D1 concentration at HLi) / D1 concentration at HL.

D1 resynthesis, as previously said, is always happening even at LL (20% in experiment 1 and 32% in experiment 2), but in high light it spikes to values of 88% and 85%, respectively, demonstrating the high degradation rates that the D1 protein suffers. One-way ANOVA followed by Tukey test shows significant differences between LL and HL treatments ($P<0.001$). How these values relate to quantum yield and other photoprotective mechanisms was the next step. Next pigment profiles and variations among treatments are described, followed by the respective quantum yields of PSII.

Pigment profiles and dynamics

HPLC was employed to check if the pigment profile was in accordance with what would be expected from photodamage induced changes described in literature. Chromatograms were obtained for each replicate of all treatments and peak areas per each pigment at the right wavelengths were used to determine pigment concentration. A typical chromatogram is shown in Fig. 17, both for low light treatments (a) and high light stress (b).

a)

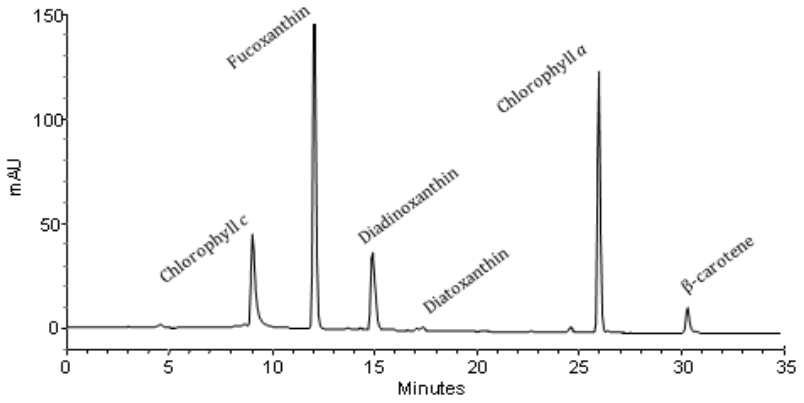

b)

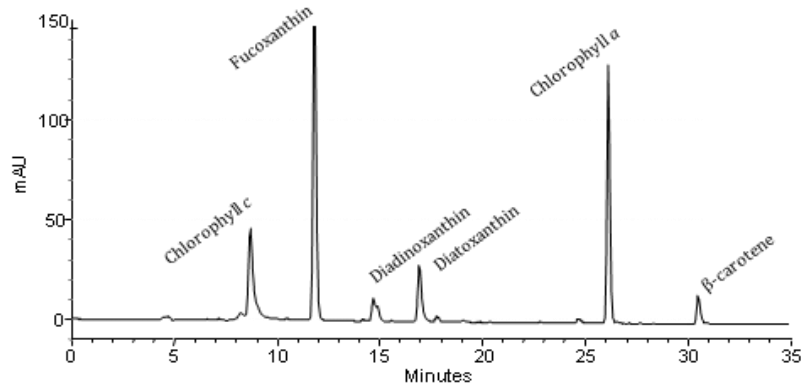

Figure 17 – HPLC chromatograms at 440 nm of pigment contents in *P. tricornutum*. 2 treatments shown: a) LL (low light, 40 µmol photons.m^{-2}.s^{-1}); and b) HL (high light, 1,250 µmol photons.m^{-2}.s^{-1}).

The chromatograms show the major pigment found in diatoms (fucoxanthin), along with the other characteristic pigment, chlorophyll *c*2. The most prominent difference in each graphic is the rise in diatoxanthin during high light induced stress, showing the mechanism of de-epoxidation is happening as a mean of protection from photodamage. These changes in epoxidation states of the xanthophylls cycle were quantified to determine the de-epoxidation state (DES). First experiments were done in different conditions, from 1 h to 3 h of high light treatment and using different light intensities, for trying to understand which conditions were worth being studied, referring to time of stress inducement and light intensity. As was observed, there weren't huge differences from 1 h to 3 h and for each light intensity, from a high light treatment of 400 µmol photons.m^{-2}.$s^{-1}$to 1250 µmol photons.m^{-2}.s^{-1} (70 ± 0.02 % and 77.4 ± 0.03 % DES, respectively, 10.4 ± 0.05 % in LL),and so the 1 h regime at 1250

µmol photons.m^{-2}.s^{-1} was adopted. The previously designated medium light of 400µmol photons.m^{-2}.s^{-1} was thus rejected, and attention focused on the higher intensity. In any case, *P. tricornutum* has a similar level of de-epoxidized xanthophylls at both light intensities. The designated final experiment, in the same conditions as cultures collected for the western immunoblotting, allowed for quantification of each of the epoxidation states of the diatom's xanthophylls, diadinoxanthin and diatoxhanthin (Table III) and the correspondent de-epoxidation state (DES, Fig. 18). Results for pigment concentrations are expressed by cell density. Cell counts were conducted using a Neubauer improved haemacytometer, counting eight medium squares, corresponding to a volume of 0.004 mm^3 each. The following formula was used to calculate density of cultures: cell concentration in culture = (number of cells counted x dilution factor) / (number of medium squares counted x area of squares x height). Cell density values were used as to control replicates and for determination of pigment concentration in pg/cell. Pigment concentrations and significant differences tested using two-way ANOVA are depicted in Table III.

Table III – Mean pigment concentration in pg/cell. Different letters indicate significant differences using two-way ANOVA followed by Tukey test ($P < 0.05$; n=4):

Pigment concentration (pg/cell)				
	LL		HL	
	Control	Inhibited	Control	Inhibited
Chl *a*	0.37 [a]	0.35 [a]	0.35 [a]	0.34 [a]
Fucoxanthin	0.21 [a]	0.20 [a]	0.20 [a]	0.18 [a]
Chl *c2*	0.07 [a]	0.07 [a]	0.07 [a]	0.06 [a]
β-carotene	0.016 [a]	0.013 [a]	0.014 [a]	0.014 [a]
DD	0.041 [a]	0.041 [a]	0.017 [b]	0.015 [b]
DT	0.0013 [a]	0.0014 [a]	0.029 [b]	0.031 [b]
DD+DT	0.043 [a]	0.043 [a]	0.046 [b]	0.046 [b]
(DD+DT)/Chl *a*	0.115 [a]	0.123 [a]	0.133 [b]	0.136 [b]

DD values are similar in both LL treatments ($4.1x10^{-2} \pm 3.3x10^{-3}$ pg/cell and $4.1x10^{-2} \pm 2.6x10^{-3}$ pg/cell, respectively) and DT values are very low ($1.3x10^{-3} \pm 4.5x10^{-4}$ pg/cell and $1.4x10^{-4} \pm 5.1x10^{-4}$ pg/cell). In HL, DD concentrations decrease more than half to $1.7x10^{-2} \pm 2.6x10^{-3}$ and $1.5x10^{-2} \pm 4.3x10^{-4}$ in LL and LLi, while DT values rise to $2.9x10^{-2} \pm 3.1x10^{-4}$

and $3.1x10^{-2}$ ± $1.9x10^{-3}$in HL and HLi. This means de-epoxidation state rises from 3.0 ± 0.89% in LL to 63.2 ± 2.2 % in HL and to 67.9 ± 2.0 % in HLi. To check if there was a constant proportion of chlorophyll to xanthophylls, (DD+DT)/Chl *a*, was calculated. Two-way ANOVA with Tukey test shows no significant differences between treatments relatively to content in fucoxanthin, Chl *c*2, Chl *a* or β-carotene. The xanthophylls (DD+DT) and their proportion to Chl *a*, however, reveal significant differences relatively to light intensity (P=0.002). There is a conversion of DD into DT, and therefore the de-epoxidation state (DES) changes. DD and DT values are significantly different between light intensities (P<0.001).

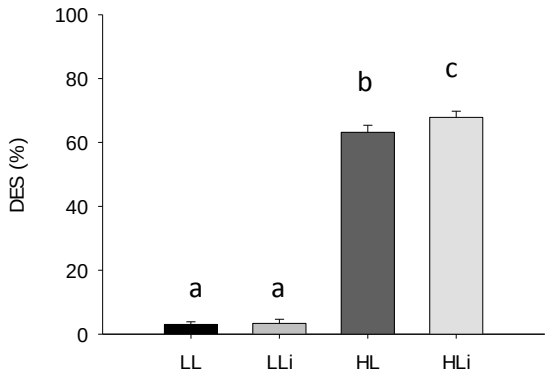

Figure 18 – De-epoxidation state [DES = DT/(DD+DT)*100] in *P. tricornutum* in the 4 treatments tested (n=4): LL (low light, 40 µmol photons.m^{-2}.s^{-1}) and HL (high light, 1,250 µmol photons.m^{-2}.s^{-1}) and same two, but with chloroplast protein synthesis inhibitor lincomycin (LLi and HLi).

Two-way ANOVA and Tukey test to DES show effect of inhibitor dependent of light (P=0.023), but only in HL (P=0.002).

Quantum yield of photosystem II during stress and repair

To study the effects of high light induced stress on photosynthetic efficiency, quantum yield of photosystem II was obtained by PAM fluorometry. Yield and NPQ = (F_m- F_m')/ F_m' profiles are shown in Fig. 19. In the dark maximum yield is obtained and when 1,250 µmol photons.m^{-2}.s^{-1} are applied, yield decreases to practically 0, and NPQ rises and keeps rising

slowly. After 1 hour, when the light is turned off, yield is recovered gradually and NPQ decreases. While NPQ reaches near null values, yield increases again, but doesn't reach its initial values. Quantum yield in HL suffers, after 24 h, a loss from 0.679 ± 0.034 to 0.557 ± 0.020, while in HLi it decreases from 0.651 ± 0.02 to 0.343 ± 0.04. NPQ rises to almost 5 both in HL and HLi, starting to decline as soon as the light is turned off (Fig. 19).

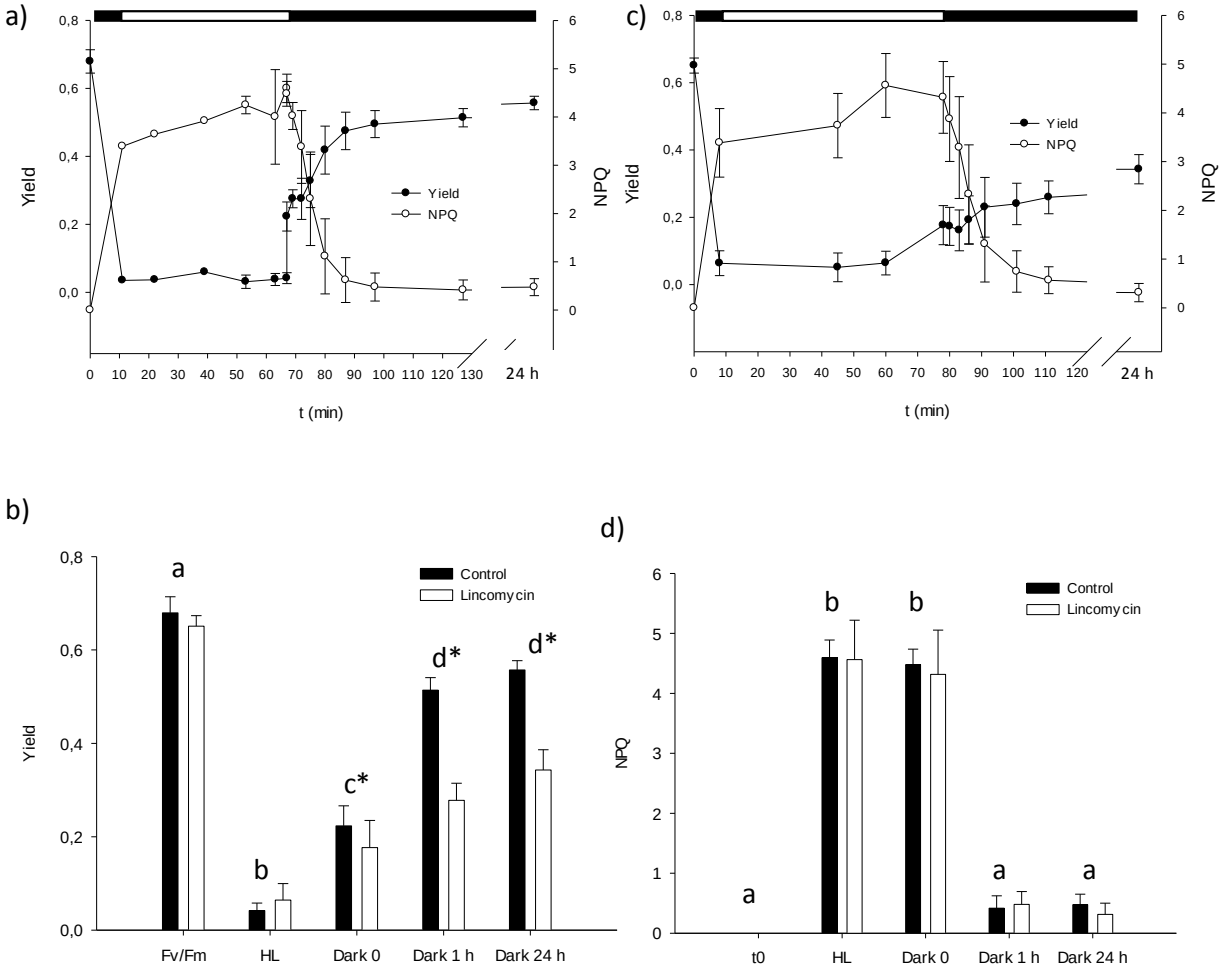

Figure 19 – Quantum yield (black dots) and NPQ (white dots) of *P. tricornutum* before, during and after inducement of 1 hour of high light stress at 1,250 µmol photons.m^{-2}.s^{-1}.a) control non-inhibited samples; (c) lincomycin inhibited samples; b) and d) represent a summary of the same results presented in vertical bars, for clarity. Different letters represent significant differences between yields at the various light intensities. * represents significant yield differences between control and inhibited cultures (n=5).

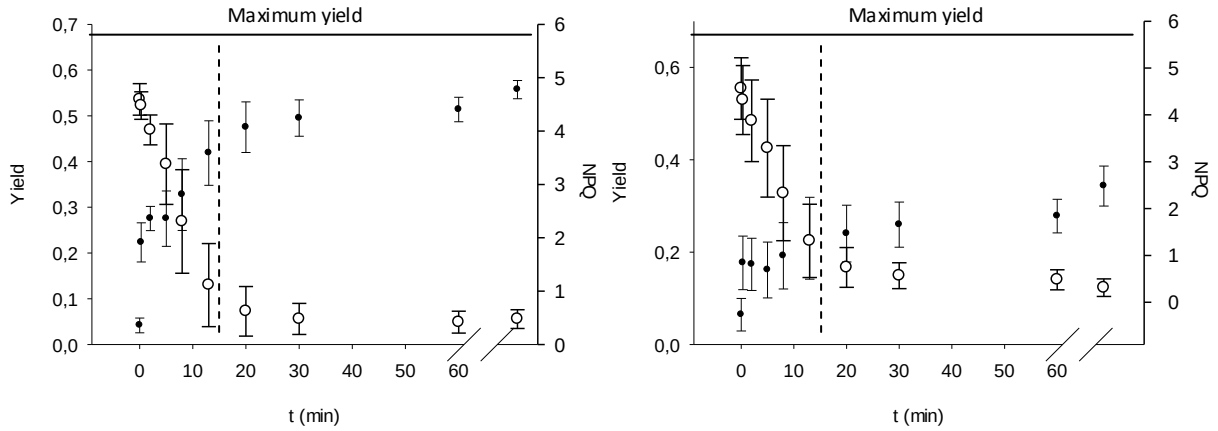

Figure 20 – Recovery kinetics of quantum yield (black dots) and NPQ (white dots) of *P. tricornutum*, after inducement of 1 hour of high light stress at 1,250 µmol photons.m^{-2}.s^{-1}. a) control, non-inhibited samples; and b) lincomycin inhibited samples. The dashed lines represent the time at which qE (to the left) ends and qI starts (to the right).

Two-way ANOVA and multiple comparisons using Tukey's test show significant differences in yield between all phases ($P<0.001$) and between control and lincomycin inhibited samples after HL ($P=0.046$ for Dark 0 and $P<0.001$ for Dark 1h and 24 h). Among control treatments there are no significant differences from 1 h in the dark to 24 h, and same goes for inhibited samples. The inhibitor has no effect on NPQ ($P=0.938$). While yield rises immediately after the light is turned off (Dark 0), to 0.223 ± 0.043 in HL and 0.177 ± 0.058 in HLi, NPQ is maintained at 4.48 ± 0.257 and 4.32 ± 0.736, respectively (Fig. 19 b and d), with $P=0.792$ between these two phases. Fast relaxation of NPQ seems occur between the 13-20 min period (Fig. 20), which correspond to dissipation of qE. From there on, qI is still present 24 h after the light is turned off (0.48 ± 0.176 in HL and 0.31 ± 0.188 in HLi). As to further infer on photoinhibition parameters and explain the variances in yield and NPQ, RLCs were used to determine maximum rETR values before and after stress was induced. E*k* is the light-saturation index, at which ETR_m occurs. α and β are the initial slope that gives photosynthetic efficiency and the photoinhibition parameter, respectively (Fig. 21).

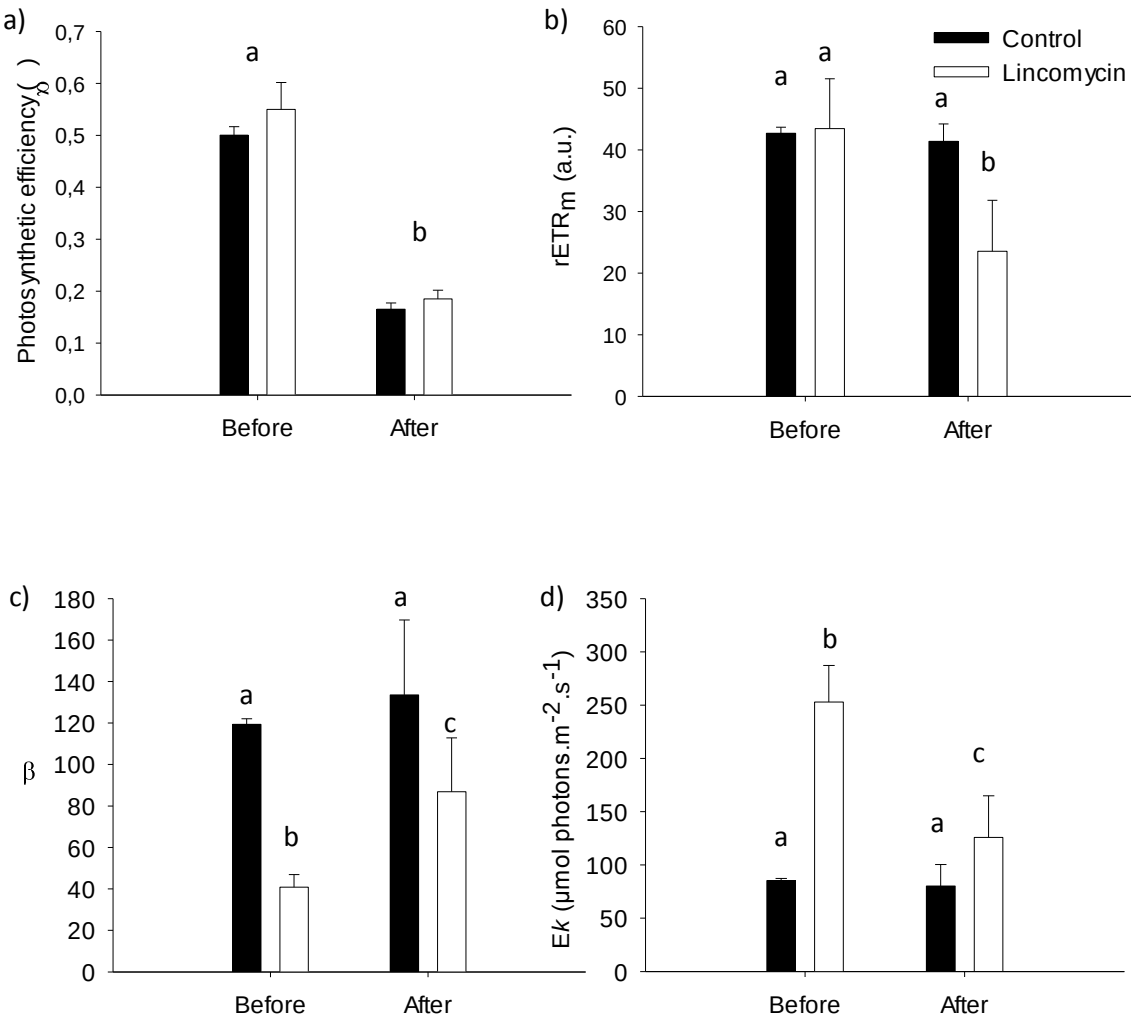

Figure 21 – RLC parameters of *P. tricornutum* before inducement of 1 hour of high light stress at 1,250 µmol photons.m^{-2}.s^{-1} and after recovery, in control and lincomycin inhibited samples (n=5). a) α; b) $rETR_m$; c) β and d) E*k*.

The initial slope of the RLCs indicates a reduction in efficiency of photosynthesis 30 min after addition of lincomycin. Two-way ANOVA shows significant difference before and after stress ($P<0.001$), but no differences in absence or presence of inhibitor ($P=0.068$). $rETR_m$ is maintained in the control HL, and decreases after recovery in HLi by half. E*k* is maintained at around 82.8 ± 3.6 µmol photons.m^{-2}.s^{-1} before and after recovery in HL, but rises to 252.8 ± 34.5 µmol photons.m^{-2}.s^{-1} before HLi stress, although it is decreased after recovery to 125.9 ± 39 µmol photons.m^{-2}.s^{-1}. Finally, a general percentage for damage to

photosynthetic activity after 24 h, calculated as $[F_v/F_m - \Phi_{PSII}$ (Dark 0)] / (F_v/F_m)*100 and recovery Φ_{PSII} (24 h) - Φ_{PSII} (Dark 0) * 100 is shown in Fig. 22.

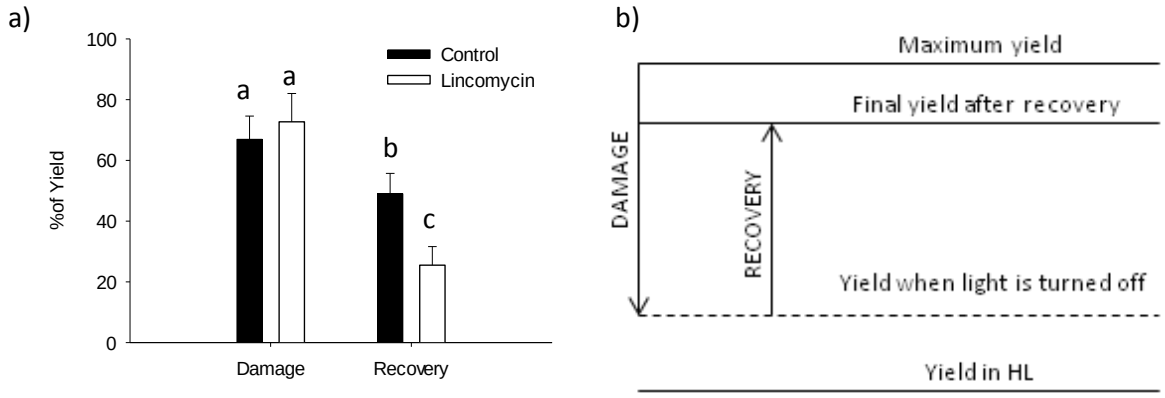

Figure 22 – Damage and recovery of quantum yield in *P. tricornutum*, after 24 h recovery of HL stress at 1,250 µmol photons.$m^{-2}.s^{-1}$, with and without chloroplast protein synthesis inhibitor lincomycin (n=5); b) scheme depicting how percentages were calculated.

One-way ANOVA on Ranks and Tukey test shows that damage is similar in both control and lincomycin treated cultures (P=0.447), but yield recovery is not (P< 0.001). Average damage in all cultures was of 69.8 ± 8.6 %, while control cultures recovered 49.0 ± 6.7 % and inhibited ones only 25.5 ± 6.1 %.

Table IV – Summary table of all main conditions analyzed for each of the 4 treatments:

	LL		HL	
	Control	Inhibited	Control	Inhibited
Yield recovery	+	+	-	--
NPQ	-	-	+	+
DES	-	-	+	+
Chl *a*	*	*	*	*
DD+DT	-	-	+	+
(DD+DT)/Chl *a*	-	-	+	+
D1 content	++	+	-	--
D1 Repair	26.2 ± 9.08 %		86.6 ± 2.36 %	

* No differences observed

Quantum yield of PSII is higher in LL and decreases only slightly when inhibitor is added (data not shown). In HL the decrease is extreme, particularly with inhibitor. NPQ has an inverse proportionality to yield and therefore is higher in HL treatments than LL, and can be as high as 5.70. DES increases in high light, existing synthesis *de novo* of DT, besides the DD pool being largely de-epoxidized to DT. D1 degradation occurred in all treatments, particularly HL and in HLi where almost no D1 is detected. Still, LLi shows that D1 is degraded even at LL. D1 repair increases from 16 % in LL to 92% in HL.

DISCUSSION

Successful and efficient extraction of D1 protein was the first main objective. There are several procedures, such as those described by Hust et al. (1999) and Janknegt et al. (2007). Essential topics to have in mind for protein extraction are the buffer pH. Serine proteases inhibitor was used (PMSF), as well as a reductant (DTT), a quelant agent (EDTA) and a detergent (Tween 20) in order to rupture membranes and solubilize proteins bound to them. It would have been preferable to use a protease inhibitor cocktail such as Exblock from BioVision (Aachen, Germany) or Sigma-Aldrich's (St. Louis, USA) protease cocktail for plants (P9599), which also inhibit metalloproteases, such as FtsH, which are known to degrade D1 efficiently, but it wasn't available and there was no money to buy it. First extraction attempts were done by grinding cells with liquid nitrogen. The efficiency of extraction was highly variable, as the room temperature was different each day, due to the absence of controlled temperature in the laboratory. The variation in extraction efficiency was troubling for Bradford quantification, as different concentration of total protein required different calibration curves, because in this case the amount of extracted proteins were on the edge of using the standard Bradford essay or the microassay, as the protein concentration would be sometimes lower, sometimes higher than 25 µg/mL, which is the critical value.

Therefore, extraction was based on sonication and freeze-thaw cycles, as it provided a more constant protein concentration per sample and a more reliable quantification. The described procedure for protein extraction provided the right amount of protein for quantification while allowing high extraction efficiency (98.2 %). Absorbance at 595 nm, and protein quantities extracted were as shown in Table 2. For determining the efficiency of protein extraction, successive extractions were performed, and when Bradford couldn't detect more protein or would detect just a residual amount, it was considered that there was no more protein to be extracted. In the 3rd successive extraction it were necessary 200 µL of extract as to detect some amount of protein, opposed to the 50 µL needed for the 1st quantification. For the SDS-PAGE, the same amounts of reagents are required to be equal, so all bands in the gels run homogeneously. There are two different types of gels put on top of each other. The top gel is a stacking gel, where HCl ions cause the totality of proteins to condense in defined bands until they reach the separation gel. Here, there is a change in pH and pore size which makes proteins migrate and separate in an easier and more defined way. Proteins can then be transferred to membranes for blotting analysis. It is needed a certain amount of total protein,

in which the specific protein that is intended to identify can be observed by binding a correct amount of antibody.

Although D1 is the major target for degradation during photodamage, other PSII components have been shown to be equally targeted for degradation, but to a lesser extent, such as D2 and CP47 (Koivuniemi et al., 1995; Aro et al., 2005). However, D1 degradation and repair is only notoriously superior to other PSII components in higher plants and green algae. In the small diatoms *Thalassiosira pseudonana* and *Conscinodiscus radiatus*, D2 appears to have a comparable turnover (Wu et al., 2011). Furthermore, when D1 is damaged, it seems to aggregate with different components such as cyt b_{559}, D2 and CP43, depending on the type and intensity of environmental stresses, *in vitro* and *in vivo* (Ohira et al., 2005). These aggregates were actually observed during the first immunoblotting trials.

The first set of our western blots showed extra bands that could be aggregates of D1/D2, D1/Cytb559 alpha subunit and others (data not shown). Ohira et al. (2005) have observed these aggregates *in vivo* in spinach leaves, and attributed them to light damage associated with higher temperatures in hot days. Diatom cultures for initial extractions were subjected to room temperature (around 25ºC), which is a stressful temperature for this strain of *P. tricornutum*, as was observed in first trials of PAM fluorometry, where photoinhibition was total after inflicting high light damage and a recovery of 24 h in the dark, all at 25ºC. These differences were also observed *in vitro* (Ishikawa et al., 1999), and further in this work when extracts weren't taken with the care needed, thus the necessity of minimizing unfreezing and always keeping them on ice when being used after extraction. Cross-linked proteins can be damaging to the cell (Ohira et al., 2005), thus these are eliminated by stroma proteases (Yamamoto et al., 2004).While it has been shown that D1 aggregation occurs both *in vivo* and *in vitro*, it seems that *P.tricornutum* might have a different D1 degradation pattern, caused by different cleavage sites, or these aggregates are only formed when stress is more severe and/or other stresses are imposed, as besides the reductant present in the extraction buffer (DTT), when β-mercaptoethanol (another reductant) wasn't added to the SDS-PAGE sample buffer, aggregates were formed, possibly indicating a tendency for these proteins to gather easily also *in vivo*.

As the blot was optimized and extraction procedures were optimized, the extra bands disappeared. What changed was a more controlled protein extraction procedure, taking care of samples carefully, always maintaining them at the lowest temperature possible, and minimizing repeated freezing after the extracts were ready for analysis. This was tried as to minimize observable bands besides D1, and it was a success. Quantification was done

immediately and extracts were put into sample buffer for protein separation by SDS-PAGE. D1 is intensely degraded during HL damage, much more than in LL, decreasing from 154 fmol.µg protein^{-1} (average of both experiments) in the latter to 78 fmol.µg protein^{-1} in the former. The repair mechanism seems to be quite effective even at HL, where 86.6 % of the protein is repaired, with repair in LL being of 26.2 %. These repair values were calculated from the values of D1 concentration with lincomycin. Wu et al. (2011) reported maximum levels of D1 in *T. pseudonana* of 47 fmol.µg protein^{-1}, while D2 was estimated in 120 fmol.µg protein^{-1}. They attributed their excess of 78 fmol.µg protein^{-1} in D2, when compared to D1, to disassembled PSII and intermediates to the repair cycle of the damaged PSII. It is a major difference from the values observed here for *P. tricornutum* in low light, which average 154 fmol.µg protein^{-1} in both experiments. However, they express their results as percentage of this initial concentration in low light, and during their white high light stress of 90 min at 1,400 µmol photons.m^{-2}.s^{-1}, D1 concentration in *T. pseudonana* decreased considerably without lincomycin (60 % of control), and to 40 % of control in the presence of lincomycin. For *C. radiatus* the levels of D1 actually increased, except when lincomycin was added, where a 30 % decrease occurred. Our results reveal that during low light, D1 is being degraded, but efficiently repaired, supported by quantum yield data. In HL D1 suffers intense degradation, which repair doesn't fully compensate for. According to Koivuniemi et al. (1995) and Rintamaki et al. (1996), D1 is dephosphorylated as a signal to degradation at the N-terminal (Elich et al., 1992). The damaged PSII complexes translocate to the stroma thylakoid membranes, if necessary. It was believed that firstly, cleavage of D1 to two 23 kDa and 10 kDa fragments (sizes of fragments differ slightly in literature) was conducted by an unknown protease (Lindahl et al., 2000), and thereafter the membrane-bound ATP-dependent zinc metalloprotease FtsH seemed to be responsible for the 23 kDa fragment proteolysis. It is now known that cleavage doesn't need to happen for FtsH proteases to act. Although there seem to be other proteases that can be involved in this matter, like DegP/HtrA proteases, it remains to be proven how necessary they are to PSII repair. The proposed cleavage sites (Edelman and Mattoo, 2008) offer an interesting interpretation of the complex dynamics and roles of the D1 protein. An explanation for the lack of shorter D1 fragments in the immunoblot is that FtsH proteases at high photoinhibitory light intensities acts solely as an endo- and exoproteinase at the N-terminal (Yoshioka and Yamamoto, 2011), in unusual stressful situations, as suggested by Edelman and Mattoo (2008), with Deg proteases acting minimally in these conditions, or then as these processes occur simultaneously, degradation is quick and no fragments are observed. It would therefore be interesting to see if different

fragments are observed if stress conditions were changed. *PsbA* transcripts in the stroma have a half-life of 10 to 40 h. In higher plants regulation is mainly conducted on translation initiation of these already present transcripts, requiring signals from both photosystems (Baena-Gonzalez and Aro, 2002). *PsbA* mRNA-ribossome complexes require light to be targeted to thylakoid membranes. Elongation and insertion into PSII complexes require that the necessary assembly factors are already present, redox control, and ligation of pigments, as well as translocation factors, such as the cpSecY channel. It was suggested a role of cpSecY/E/G translocon system in a myriad of nuclear and chloroplast encoded proteins translocation to thylakoid membranes by Baena-Gonzalez and Aro (2002) and Zhang and Aro (2002), with cpSecA chaperone probably assisting (Zhang and Aro, 2002). The removal of the C-terminal extension by CtpA (carboxyl-terminal peptidase A) restores the water-splitting activity of the OEC, as it provides a ligand to the Mn cluster (Satoh and Yamamoto, 2007). OEC proteins are separated from PSII during the repair process but aren't targeted for degradation. They stay in the lumen waiting for reassembly. These results will be further discussed after interpreting PAM fluorometry data.

Maximum quantum yield of dark-adapted chloroplasts was of 0.663, for all replicates (Fig. 19). These values decrease slightly (2.5 %, data not shown) when low light at 40 µmol photons.m^{-2}.s^{-1} is turned on. When high light stress is inflicted to cells, however, effective quantum yield goes down to 0.053. Therefore, at this light intensity photosynthesis is profoundly impaired. This happens whether lincomycin is present or not. The effect of lincomycin was seen only in recovery after the stressful light was turned off. Control samples still exhibit chronic loss of photosynthetic capacity, as 1 h after the light is turned off, yield rises back to 0.514, to a final recovery after 24 h in the dark to 0.553 (Fig. 19 a, b), corresponding to a final recovery in photosynthetic capacity of 81.5 % (Fig. 22). When lincomycin is present and no new synthesis of D1 occurs, yield is strongly affected, rising only to 0.306 after 1 h, to a final recovery 24 h after relaxation in the dark to 0.354 (Fig. 19 c, d), representing a 54.3 % recovery in quantum yield of PSII (Fig. 22). However, while photosynthesis is impaired when HL is turned on, yield actually increases to 0.223 in control samples and to 0.177 in inhibited samples, immediately after the light is turned off, indicating that almost all reaction centres are closed in HL, but not all of them are damaged. Also, D1 degradation is less severe than the effects on yield, indicative of inactive reaction centres (Leitsch et al., 1994) when the high light is on. Recovery was therefore of 49 % in HL and 26 % in HLi (Fig.22). These results can be attributed to the lowering of photochemical yield of PSII by NPQ (Wu et al., 2011). More so, inhibited cultures have further damaged PSII

complexes resulting in lower yields at this point. The relation $1/F_0 - 1/F_m$ is linearly correlated with the proportion of functional PSIIs (Wu et al., 2011). While the data was treated in order to have this information, the results showed too much variation as to be reliable, but after 1 h recovery in the dark they ranged from 60 – 80 % functional in HL and 25 to 50 % functional in HLi. During exposure to HL these values were only of 4 to 10 % in all cultures.

NPQ values rise to a peak average of 4.6 in all treatments, with the maximum value registered being 5.70. Diatoms are known to have a NPQ capacity 5-fold higher than green algae and higher plants (Nymark et al., 2009) and in *P. tricornutum* these values are generally even higher (Ruban et al., 2004). This huge NPQ dissipates energy from the reaction centres, which causes the big decrease in chlorophyll fluorescence during exposure to HL (also shown by Lavaud et al., 2002). When HL is turned off, NPQ starts decreasing slowly, eventually getting close to 0, but is sustained 24 h later, also observed by Zhu and Green (2010) in *T. pseudonana*. NPQ is constituted by two components in diatoms, qE and qI, and actually only qE and qI were observed (Fig. 20). While β-carotene provides for energy dissipation as heat in LHCs, the changes in composition to higher contents of DT provide stronger protection and probably distribute excess energy equally between the two photosystems (Nymark et al., 2009; Rochaix, 2001). The qE mechanism represents the dominating NPQ component under moderate light stress conditions and is related to energy dissipation processes generated by the energization of the thylakoid membrane (Bajkan et al., 2010; White and Critchley, 1999). It requires a proton gradient and relaxes in a matter of seconds to minutes. Leitsch et al. (1994) reported that 10 min in the dark were sufficient for qE dissipation, relatively close to the 13-20 interval we observed, where qE stops and qI starts (Fig. 20). The pH regulation of qE allows a flexible and rapid switch of the function of the PSII antenna between light harvesting and energy dissipation upon rapidly changing light conditions. qI is the photoinhibitory quenching only happening during severe damage. Its relaxation kinetics take long hours (Muller et al., 2001) and are supposed to be based on energy dissipation in the antenna of PSII, representing an efficient mechanism to reduce the electron pressure on the photosynthetic electron transport chain at saturating light intensities (Kalituho et al., 2007). This process is controlled by the synergistic action of the lumen pH, xanthophyll binding, and conformational changes in the antenna of PSII, and is only slowly (30 min to several days) reversible due to the requirement of turnover of the D1 protein and DT epoxidation by DT epoxidase (Muller et al., 2001; White and Critchley, 1999). The qI quenching is related to photoinhibition of photosynthesis and develops upon prolonged exposure of chloroplasts to highly excessive light stress conditions. However, the nature of qI is not fully clear. To further

confirm changes in photosynthetic activity, pigment profiles and concentrations were determined using HPLC. Major pigments such as Chl *a*, *c*2 and fucoxanthin remained at constant concentrations in all 4 treatments (Table 3 and Fig. 18). The addition of inhibitor didn't cause any variation in these pigments, both in LL and HL. There was transformation of DD in DT, as DD in LL averages 0.041 pg/cell and decreases to 0.016 pg/cell. Some DD molecules are bound to membrane lipids, while the majority is bound to FCP proteins together with fucoxanthin, Chl *a* and *c*. The membrane association is essential for diadinoxanthin de-epoxidase function (Bertrand, 2010). As DD is converted in DT by DD de-epoxidase, DT concentrations rise from 0.0014 pg/cell to 0.03 pg/cell. However, synthesis *de novo* of DT also occurs. Fucoxanthin is a precursor of diadinoxanthin (Bertrand, 2010), but as fucoxanthin values didn't suffer any alteration, it can only mean that DT was synthesized *de novo*, with no use of the already present fucoxanthin molecules. The proportion of xanthophylls relatively to Chl *a* rises in HL to 0.130, from 0.119 in LL. β-carotene also remains constant, although some authors have already observed increases of 15 % in the content of this pigment in higher plants (Depka et al., 1998). Thus, the only relevant change in pigment profiles was the increase in DT in HL treatments, with *de novo* synthesis occurring and NPQ rising. The de-epoxidation state, DES (Fig. 18), is 3.17 % in LL and in HL 65.51 %.

RLCs allowed for estimation of ETR_m and initial slope, α (Fig. 21 a, b). The slope is indicative of the efficiency of photosynthesis. The higher the slope, the more of the absorbed photons are used and converted in photochemical energy, and vice-versa. In both HL measurements (control and with lincomycin), α is 0.50 and 0.55 before stress, respectively, with the efficiency decreasing to 0.165 and 0.185, 1 h after HL recovery. While there is no significant difference in the efficiency among control and inhibited cultures, the ETR_m declines significantly with inhibitor, from 43.5 to 23.5, while in control samples ETR_m remains almost the same (43 to 41 after stress). This in itself is further indicative of the damaged D1 interrupting correct electron transport almost by half, if PSII isn't repaired by replacement of the damaged D1 pool. However, there seems to be another reason for the decrease in yield besides the electron transport being affected, as recovery in HL samples was not total, although the $rETR_m$ is largely unchanged. β and E*k* (Fig. 21 c, d) represent the photoinhibition parameter and the light intensity at which ETR_m is reached, respectively. Nymark et al. (2009) observed a $rETR_m$ superior to 30 after being exposed for 1h to both LL (35 µmol photons.m^{-2}.s^{-1}) and HL at 500 µmol photons.m^{-2}.s^{-1}. However, they do get higher $rETR_m$ 24 h later and even higher 48 h later. Other species actually have higher $rETR_m$ at temperatures above 15ºC, decreasing only after the 25ºC are surpassed (Yun et al., 2010), but

our data (not shown) suggest *P. tricornutum* is very sensitive to temperatures higher than 15ºC. Although in this study by Nymark et al. (2009) cultures only had 3 min to adapt to the dark after exposure, and there was no study on the effect of inhibition of protein synthesis, it is indicative of a highly efficient acclimation mechanism. Interestingly, E*k* is quite low when *P. tricornutum* cultures are dark-adapted after being grown at LL conditions (83 µmol photons.m^{-2}.s^{-1}), but after approximately 40 min of addition of the inhibitor E*k* rises tremendously. After stress and 24 h recovery, however, photoinhibition occurs at a lower light intensity, where protein synthesis was inhibited. In HLi samples before stress (corresponding to LLi, as cultures were at 40 µmol photons.m^{-2}.s^{-1} prior to fluorescence measurements), E*k* rised to 253 µmol photons.m^{-2}.s^{-1}, while after recovery of HLi, this value decreases by half to 126 µmol photons.m^{-2}.s^{-1}. With the inhibitor, considering the $rETR_m$ is lower, less light is required for it to be achieved, thus the lower E*k*. Nymark et al. (2009) report an E*k* superior to 200 µmol photons.m^{-2}.s^{-1} after being exposed 24 h to HL 500 µmol photons.m^{-2}.s^{-1}, although in the first hour it remains relatively unchanged at 100 µmol photons.m^{-2}.s^{-1}. These authors also measured parameters for LL-grown cultures (35 µmol photons.m^{-2}.s^{-1}) where E*k* was maintained for 48 h at approximately 100 µmol photons.m^{-2}.s^{-1}. Actually, LL cultures' $rETR_m$ and E*k* remained relatively unchanged. Thus, while the values obtained by Nymark et al. (2009) in LL are 20% higher, the HL values for E*k* at 48 h are similar to our inhibited samples before stress. Our data is contradicted as they show a constant increase in ETR_m and E*k* during the 48 h. It would be interesting to see what would have happened had the authors allowed the cultures to adapt to the dark and recover for a longer period of time, as to further study the influence of the time of exposure to stress. Is it necessary to be exposed to HL for 24 h or 48 h and the photoprotection capacity grows with it, maybe translating into a photoacclimation response? Or maybe just 1 h of exposure induces gradual change, or a stronger response the stronger the irradiated light is, that although not as efficient, provides further protection to stressful conditions.

Efficiency can be lower, because of other variables not accounted for with the model used. If the slope is high, but there is a long curvature following it before the ETR_m is achieved, E*k* will be higher. Efficiency should also be proportional to ETR_m, but that wasn't observed in HL cultures after recovery, where efficiency is lower, but ETR_m is maintained and E*k* is the highest. What is happening is that in HL, probably because of the damaged PSIIs, photosynthetic efficiency diminishes, thus being required more light to achieve ETR_m.

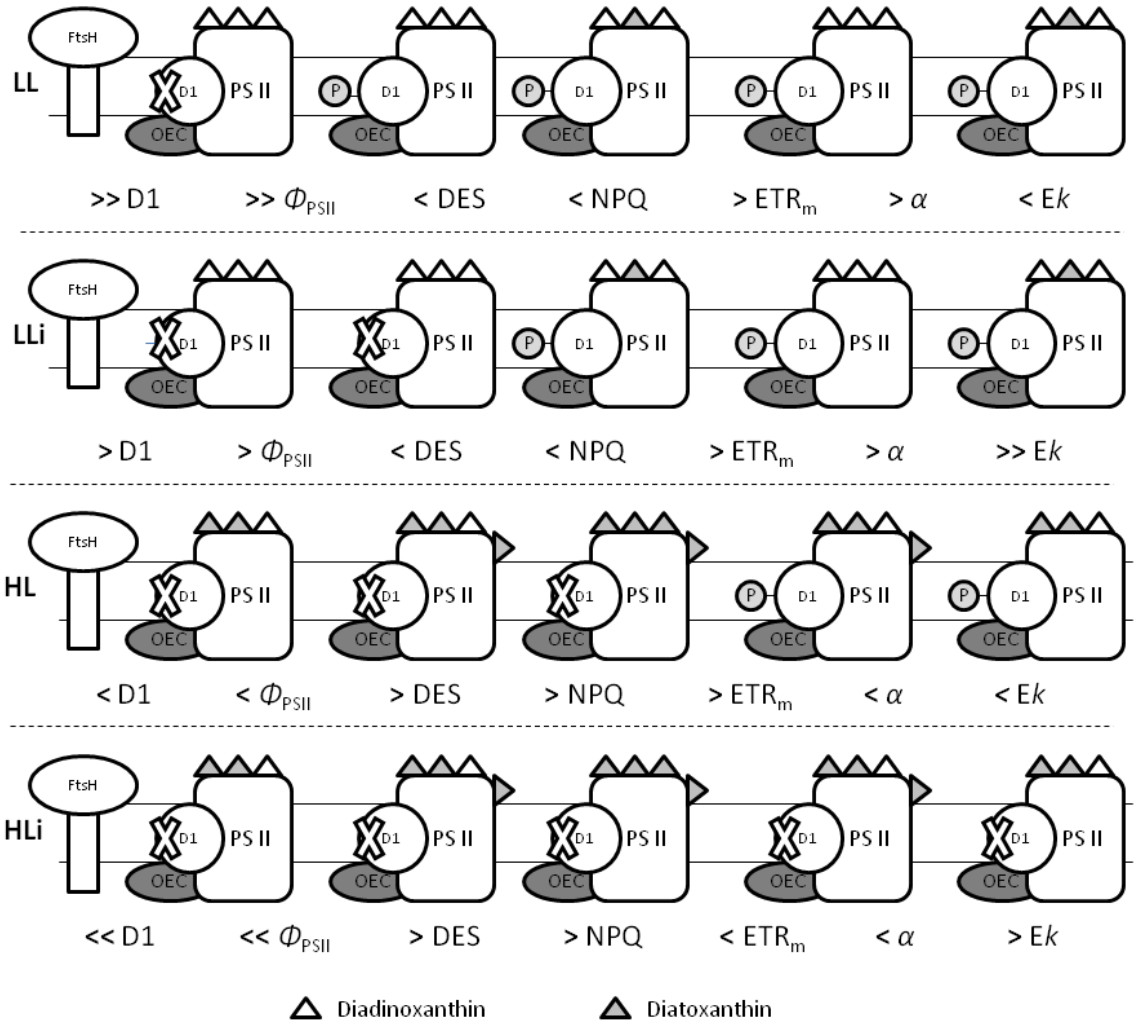

Figure 23 – Summary schematics of data obtained with all methodologies employed.

Other environmental stresses other than strong light seem to inhibit repair of PSII (Murata et al., 2007), including heat and cold stress, high salinity and CO_2 limitation. This rises ROS formation and consequently further inhibit the repair of PSII components, mainly D1 (Takahashi and Murata, 2008). Several works evidence $^1O_2$ as the most damaging ROS during photoinhibition (Krieger-Liszkay, 2005), at least in *Chlamydomonas reinhardtii* and in *Arabidopsis thaliana*. Limitation of CO_2 fixation decreases ATP and NADPH consumption, especially in high light conditions (Takahashi and Murata, 2008). Other relevant damaging ROS is H_2O_2, which is normally reduced by electrons coming from PSI or by peroxidase (Takahashi and Murata, 2008). If ROS are not scavenged, they are free to interfere with repair, by inactivating elongation factor G (EF-G), which elongates the D1 protein. Another example is the Rubisco of higher plants. It is stable under warmer temperatures, although its

activase isn't, thus accelerating H_2O_2 production by carbon limitation under heat, inhibiting repair (Murata et al., 2007). Furthermore, recently the primary target of photodamage was found to be the OEC, particularly the Mn cluster, with release of manganese ions, consequent inactivation of the OEC and high formation of endogenous radical $P680^+$ (Henmi et al., 2004; Murata et al., 2007; Tyystjärvi, 2008). Mechanisms for production and depletion of ROS are described thoroughly by Pospisil (2011).

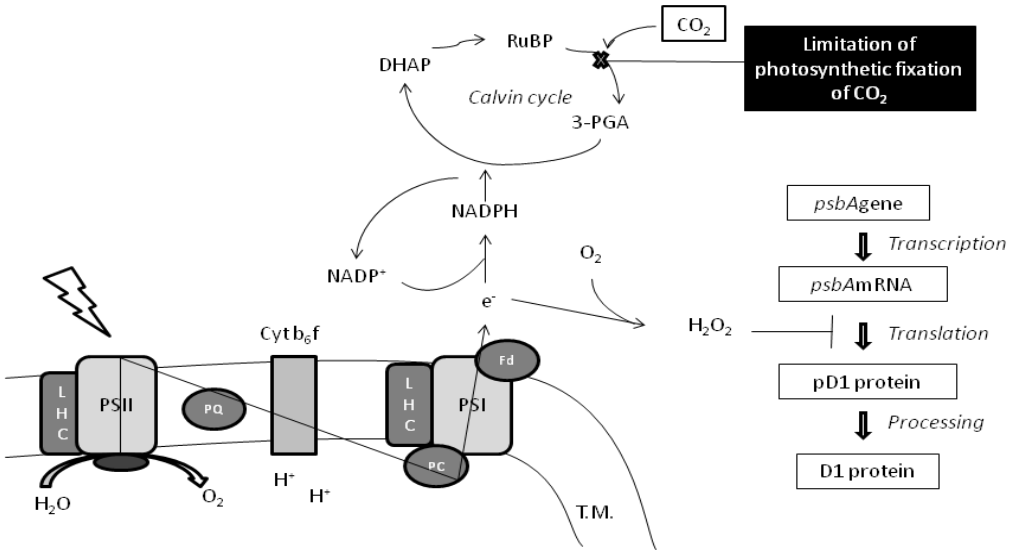

Figure 24 – Inhibition of repair by carbon limitation, adapted from Takahashi and Murata (2008). DHAP is dihydroxyacetone phosphate; 3-PGA is 3-phosphoglyceric acid and RuBP is ribulose-1,5-bisphosphate.

The proportion at which the damage/repair processes occur, results in different photoacclimation characteristics. While the extreme NPQ values of *P. tricornutum* dissipate photochemical energy from the reaction centres, resulting in very low PSII yields, there are still many functional PSIIs, which open immediately upon turning off the light, or turning the light back to growth intensity. The high variability observed can be attributed to the ability of photosynthesis to respond broadly to different stimuli, as photosynthesis itself originates signals for acclimation, with unicellular autotrophs using the redox signals to induce responses (Walters, 2005).

Summarizing, as light hits pigments and photochemical energy is formed, some reaction centres close, meaning they cannot receive e^-. The energy of the photons excess has to be dissipated and it is as fluorescence or heat. Fluorescence emission rises, as well as dissipation as heat (NPQ), as some DD s are de-epoxidized to DT. At the same time, D1 still suffers some damage from its constant activity and because of e^- that escape the photosynthetic chain, either in Q_A, by charge recombination with $Pheo^-$, triplet P680 chlorophyll *a* formation, Q_A^{2-} or Q_AH_2. These will further produce ROS which will inhibit repair of PSII units. These mechanisms, however, are only relevantly damaging when light is in excess. This is because the ROS that are formed are scavenged efficiently in normal light, but when light is saturating, all reaction centres may be closed, and more highly reactive damaging molecules are produced. Thus there are more photons being reemitted as fluorescence, therefore decreasing photochemical energy, protecting saturated reaction centres. This results in almost null quantum yields, explained also by the extremely high NPQs in *P. tricornutum*. Stressful HL causes a prolonged exposure of D1 and other PSII subunits to the damaging molecules. Mainly triplet P680, $P680^+$ and tyr_Z^+ seem to affect directly D1, while ROS seem to action on proteins involved in protein translation, like elongation factors such as EF-G. The repair of PSII is highly affected in HL, supported by the high loss in D1 concentration. If protein synthesis is inhibited, however, the damage is also noticed in LL, and in HL almost no D1 protein is detected. So, why the yields are so greatly recovered after HL stress can only be explained by an unknown phenomenon occurring, or simply because D1 degradation is occurring in excess in the eppendorfs, because there is FtsH present, as the inhibitor present (PMSF) does not inhibit metalloproteases. This degradation could occur if samples were subjected to a temperature at which FtsH was activated, presuming other factors such as pH were also ideal. This means there would probably be more D1 in the LL control treatment, and therefore the concentrations, being as high as they are when compared with other described values for other species, were sub estimated. It is however still clear, that light is profoundly damaging to the D1/psbA protein, and that if repair is inhibited, severe photoinhibition will occur.

FUTURE PERSPECTIVES

Research on the D1 protein will remain abundant while the mechanisms underlying photosynthesis aren't fully comprehended. While the data obtained in this work is valuable, there are still things that could have been done better and starting points for further investigation. Trying different light intensities at lower and higher temperatures or infliction of other stressful abiotic factors would be of interest as to check for different effects on the D1 protein and photosynthetic activity of PSII. The formation of dimmers and other aggregates of the D1 protein with other PSII constituents under different stressful events could be indicative of different physiological status. There are already D1 mutants of *P. tricornutum* (Materna et al. 2009). These mutant strains can reveal more about the different activities that the D1 protein and specific regions if the protein can exert. It should also be considered the use of a reference protein which is known not to suffer variation in content, to serve as reference for the quantity of D1. Studying *psbA* transcripts could provide more precise information about repair and turnover processes and rates. Variations in other PSII subunits, namely psbD (D2) and psbB (CP43) should be accounted for. For PAM fluorometry to be more elucidative, different acclimation phases should be checked, with measurements conducted through 48 h after light exposure and search for differences in different times of exposure to different light intensities, and the effect on D1 content and state. NPQ development should also be studied more thoroughly, as data obtained suggest slower NPQ formation as an effect of the inhibitor. Whether this is an indirect side effect, completely unrelated to what happens *in vivo*, should be resolved. And preferably, a Water-PAM should be used. It would be interesting to run samples on high resolution or bigger gels, to enable distinction of phosphorylated or dephosphorylated D1 and its ratios. Malondialdehyde (MDA) should be used to quantify ROS formation. Oxygen flash yields could be used to track functional PSII, as the linear relation used was not elucidative or reliable. As it has been observed that *P. tricornutum* is a particularly resistant species to stress, comparing these with other supposedly less adapted species of diatoms could prove special adaptations of this species and its potential and importance for the ecosystems. The procedures developed in this thesis are intended for observation of D1 degradation *in situ* in microalgae living in the benthos of intertidal habitats. These communities are composed mainly by diatom species, such as several *Navicula*, *Gyrosigma* and *Nitzschia* species. As *P. tricornutum* is mainly planktonic, it's interesting that sometimes they are found in benthonic communities, where it

seems the oval form is predominant (Johansen, 1991), while triradiate and fusiform cells are mainly planktonic forms. The strain used in this work was oval, and actually sometimes it would adhere to the bottom of the flasks where it was grown, but normally it was planktonic. Furthermore, sometimes the triradiate form was observed, especially after HL stress. It is revealing of some morphological plasticity by *P. tricornutum*. Are these mechanisms of adaptation? And what for? Did these strains develop any special characteristics for this habitat? Do all the benthonic diatoms have these adaptations? Maybe the high NPQ rates derived from a need to be in the soil and protect to the high irradiances that they are subjected to when tides are low or the soil is exposed to the air. The high efficiencies of carbon fixation by diatoms and their capacity for recovery are invaluable. These questions remain unanswered and necessitate further research. Comparing strains that live in that same habitat and exhibit completely different behaviours, photosynthetic, photoprotection and photoacclimation processes, compare this information with genome data can provide explanations for why some species are stronger than others, and even explain the intraspecific differences.

REFERENCES

Anemaet, I.G., Bekker, M., and Hellingwerf, K.J. (2010). Algal photosynthesis as the primary driver for a sustainable development in energy, feed, and food production. Mar Biotechnol (NY) *12*, 619-629.

Armbrust, E.V. (2009). The life of diatoms in the world's oceans. Nature *459*, 185-192.

Armbrust, E.V., Berges, J.A., Bowler, C., Green, B.R., Martinez, D., Putnam, N.H., Zhou, S., Allen, A.E., Apt, K.E., Bechner, M., *et al.* (2004). The genome of the diatom Thalassiosira pseudonana: ecology, evolution, and metabolism. Science *306*, 79-86.

Aro, E.M., Suorsa, M., Rokka, A., Allahverdiyeva, Y., Paakkarinen, V., Saleem, A., Battchikova, N., and Rintamaki, E. (2005). Dynamics of photosystem II: a proteomic approach to thylakoid protein complexes. J Exp Bot *56*, 347-356.

Baena-Gonzalez, E., and Aro, E.M. (2002). Biogenesis, assembly and turnover of photosystem II units. Philos Trans R Soc Lond B Biol Sci *357*, 1451-1460.

Bajkan, S., Varadi, G., Balogh, M., Domonkos, A., Kiss, G.B., Kovacs, L., and Lehoczki, E. (2010). Conserved structure of the chloroplast-DNA encoded D1 protein is essential for effective photoprotection via non-photochemical thermal dissipation in higher plants. Mol Genet Genomics *284*, 55-63.

Barber, J. (2008). Crystal structure of the oxygen-evolving complex of photosystem II. Inorg Chem *47*, 1700-1710.

Barber, J., and Kuhlbrandt, W. (1999). Photosystem II. Curr Opin Struct Biol *9*, 469-475.

Belshe, E.F., Durako, M.J., and Blum, J.E. (2007). Photosynthetic rapid light curves (RLC) of *Thalassia testudinum* exhibit diurnal variation. J Exp Mar Biol Ecol *342*, 253-265.

Bertrand, M. (2010). Carotenoid biosynthesis in diatoms. Photosynth Res *106*, 89-102.

Bonardi, V., Pesaresi, P., Becker, T., Schleiff, E., Wagner, R., Pfannschmidt, T., Jahns, P., and Leister, D. (2005). Photosystem II core phosphorylation and photosynthetic acclimation require two different protein kinases. Nature *437*, 1179-1182.

Bowler, C., Karl, D.M., and Colwell, R.R. (2009). Microbial oceanography in a sea of opportunity. Nature *459*, 180-184.

Bozarth, A., Maier, U.G., and Zauner, S. (2009). Diatoms in biotechnology: modern tools and applications. Appl Microbiol Biotechnol *82*, 195-201.

Cartaxana, P., and Serôdio, J. (2008). Inhibiting diatom motility: a new tool for the study of the photophysiology of intertidal microphytobenthic biofilms. Limnol and Oceanogr: Methods *6*, 11.

Depka, B., Jahns, P., and Trebst, A. (1998). Beta-carotene to zeaxanthin conversion in the rapid turnover of the D1 protein of photosystem II. FEBS Lett *424*, 267-270.

Edelman, M., and Mattoo, A.K. (2008). D1-protein dynamics in photosystem II: the lingering enigma. Photosynth Res *98*, 609-620.

Elich, T.D., Edelman, M., and Mattoo, A.K. (1992). Identification, characterization, and resolution of the in vivo phosphorylated form of the D1 photosystem II reaction center protein. J Biol Chem *267*, 3523-3529.

Falkowski, P.G., Katz, M.E., Knoll, A.H., Quigg, A., Raven, J.A., Schofield, O., and Taylor, F.J. (2004). The evolution of modern eukaryotic phytoplankton. Science *305*, 354-360.

Falkowski, P.G., and Raven, J.A. (1997). Aquatic photosynthesis (USA, Blackwell Science).

Finazzi, G., Rappaport, F., and Goldschmidt-Clermont, M. (2003). From light to life: an interdisciplinary journey into photosynthetic activity. EMBO Rep *4*, 752-756.

Govindjee (1995). Sixty-three years since Kaustky: Chlorophyll *a* fluorescence. Australian Journal of Plant Physiology *22*, 131-160.

Greenwell, H.C., Laurens, L.M., Shields, R.J., Lovitt, R.W., and Flynn, K.J. (2010). Placing microalgae on the biofuels priority list: a review of the technological challenges. J R Soc Interface *7*, 703-726.

Halim, R., Gladman, B., Danquah, M.K., and Webley, P.A. (2011). Oil extraction from microalgae for biodiesel production. Bioresource Technol *102*, 178-185.

Henmi, T., Miyao, M., and Yamamoto, Y. (2004). Release and reactive-oxygen-mediated damage of the oxygen-evolving complex subunits of PSII during photoinhibition. Plant Cell Physiol *45*, 243-250.

Horton, P., and Ruban, A. (2005). Molecular design of the photosystem II light-harvesting antenna: photosynthesis and photoprotection. J Exp Bot *56*, 365-373.

Hust, M., Krumbein, W.E., and Rhiel, E. (1999). An immunochemical in situ approach to detect adaptation processes in the photosynthetic apparatus of diatoms of the Wadden Sea sediment surface layers. J Microbiol Methods *38*, 69-80.

Ishikawa, Y., Nakatani, E., Henmi, T., Ferjani, A., Harada, Y., Tamura, N., and Yamamoto, Y. (1999). Turnover of the aggregates and cross-linked products of the D1 protein generated by acceptor-side photoinhibition of photosystem II. Biochim Biophys Acta *1413*, 147-158.

Janknegt, P.J., Rijstenbil, J.W., van de Poll, W.H., Gechev, T.S., and Buma, A.G. (2007). A comparison of quantitative and qualitative superoxide dismutase assays for application to low temperature microalgae. J Photochem Photobiol B *87*, 218-226.

Johansen, J.R. (1991). Morphological variability and cell wall composition of *Phaeodactylum tricornutum* (Baccillariophyceae). Great Basin Nat *51*(4), 310-315.

Kalituho, L., Beran, K.C., and Jahns, P. (2007). The transiently generated nonphotochemical quenching of excitation energy in Arabidopsis leaves is modulated by zeaxanthin. Plant Physiol *143*, 1861-1870.

Kettunen, R., Tyystjarvi, E., and Aro, E.M. (1991). D1 protein degradation during photoinhibition of intact leaves. A modification of the D1 protein precedes degradation. FEBS Lett *290*, 153-156.

Kilian, O., Steunou, A.S., Grossman, A.R., and Bhaya, D. (2008). A novel two domain-fusion protein in cyanobacteria with similarity to the CAB/ELIP/HLIP superfamily: evolutionary implications and regulation. Mol Plant *1*, 155-166.

Kitajima, M., and Butler, W.L. (1975). Quenching of chlorophyll fluorescence and primary photochemistry in chloroplasts by dibromothymoquinone. Biochim Biophys Acta *376*, 105-115.

Klimov, V.V., and Baranov, S.V. (2001). Bicarbonate requirement for the water-oxidizing complex of photosystem II. Biochim Biophys Acta *1503*, 187-196.

Koivuniemi, A., Aro, E.M., and Andersson, B. (1995). Degradation of the D1- and D2-proteins of photosystem II in higher plants is regulated by reversible phosphorylation. Biochemistry *34*, 16022-16029.

Kooten, O., and Snel, J.F.H. (1990). The use of chlorophyll fluorescence nomenclature in plant stress physiology. Photosynth Res *25*, 147-150.

Krieger-Liszkay, A. (2005). Singlet oxygen production in photosynthesis. J Exp Bot *56*, 337-346.

Lang, M., and Kroth, P.G. (2001). Diatom fucoxanthin chlorophyll a/c-binding protein (FCP) and land plant light-harvesting proteins use a similar pathway for thylakoid membrane Insertion. J Biol Chem *276*, 7985-7991.

Lavaud, J., Rousseau, B., van Gorkom, H.J., and Etienne, A.L. (2002). Influence of the diadinoxanthin pool size on photoprotection in the marine planktonic diatom *Phaeodactylum tricornutum*. Plant Physiol *129*, 1398-1406.

Lavaud, J., Strezpek, R.F., and Kroth, P.G. (2007). Photoprotection capacity differs among diatoms: Possible consequences on the spatial distribution of diatoms related to fluctuations in the underwater light climate. Limnol Oceanogr *52*, 1188-1194.

Leitsch, J., Schnettger, B., Critchley, C., and Krause, G.H. (1994). Two mechanisms of recovery from photoinhibition *in vivo*: reactivation of photosystem II related and related to D1-protein turnover. Planta *194*, 15-20.

Lindahl, M., Spetea, C., Hundal, T., Oppenheim, A.B., Adam, Z., and Andersson, B. (2000). The thylakoid FtsH protease plays a role in the light-induced turnover of the photosystem II D1 protein. Plant Cell *12*, 419-431.

Materna, A.C., Sturm, S., Kroth, P.G., and Lavaud, J. (2009). First induced plastid genome mutations in an alga with secondary plastids: *psb*A mutation in the diatom *Phaeodactylum tricornutum* (Bacillariophyceae) reveal consequences on the regulation of photosynthesis. J Phycol *45*, 838-846.

Montane, M.H., and Kloppstech, K. (2000). The family of light-harvesting-related proteins (LHCs, ELIPs, HLIPs): was the harvesting of light their primary function? Gene *258*, 1-8.

Muller, P., Li, X.P., and Niyogi, K.K. (2001). Non-photochemical quenching. A response to excess light energy. Plant Physiol *125*, 1558-1566.

Murata, N., Takahashi, S., Nishiyama, Y., and Allakhverdiev, S.I. (2007). Photoinhibition of photosystem II under environmental stress. Biochim Biophys Acta *1767*, 414-421.

Napiwotzki, A., Bergmann, A., Decker, K., Legall, H., Eckert, H.J., Eichler, H.J., and Renger, G. (1997). Acceptor side photoinhibition in PS II: On the possible effects of the functional integrity of the PS II donor side on photoinhibition of stable charge separation. Photosynth Res *52*, 199-213.

Nelson, N., and Yocum, C.F. (2006). Structure and function of photosystems I and II. Annu Rev Plant Biol *57*, 521-565.

Nixon, P.J., Michoux, F., Yu, J., Boehm, M., and Komenda, J. (2010). Recent advances in understanding the assembly and repair of photosystem II. Ann Bot *106*, 1-16.

Nymark, M., Valle, K.C., Brembu, T., Hancke, K., Winge, P., Andresen, K., Johnsen, G., and Bones, A.M. (2009). An integrated analysis of molecular acclimation to high light in the marine diatom *Phaeodactylum tricornutum*. PLoS One *4*, 1-14.

Ohira, S., Morita, N., Suh, H.J., Jung, J., and Yamamoto, Y. (2005). Quality control of photosystem II under light stress - turnover of aggregates of the D1 protein *in vivo*. Photosynth Res *84*, 29-33.

Pantazis, D.A., Orio, M., Petrenko, T., Zein, S., Lubitz, W., Messinger, J., and Neese, F. (2009). Structure of the oxygen-evolving complex of photosystem II: information on the S(2) state through quantum chemical calculation of its magnetic properties. Phys Chem Chem Phys *11*, 6788-6798.

Pieters, A.J., Tezara, W., and Herrera, A. (2003). Operation of the xanthophyll cycle and degradation of D1 protein in the inducible CAM plant, *Talinum triangulare*, under water deficit. Ann Bot *92*, 393-399.

Platt, T., and Jassby, A.D. (1976). The relationship between photosynthesis and light for natural assemblages of coastal marine phytoplankton. J Phycol *12*, 421-430.

Pospisil, P. (2011). Molecular mechanisms of production and scavenging of reactive oxygen species by photosystem II. Biochim Biophys Acta.

Renger, G. (2001). Photosynthetic water oxidation to molecular oxygen: apparatus and mechanism. Biochim Biophys Acta *1503*, 210-228.

Rintamaki, E., Kettunen, R., and Aro, E.M. (1996). Differential D1 dephosphorylation in functional and photodamaged photosystem II centers. Dephosphorylation is a prerequisite for degradation of damaged D1. J Biol Chem *271*, 14870-14875.

Rochaix, J.D. (2001). Assembly,function, and dynamics of the photosynthetic machinery in *Chlamydomonas reinhardtii*. Plant Physiol *127*, 1394-1398.

Ruban, A., Lavaud, J., Rousseau, B., Guglielmi, G., Horton, P., and Etienne, A.L. (2004). The super-excess energy dissipation in diatom algae: comparative analysis with higher plants. Photosynth Res *82*, 165-175.

Ruban, A.V., and Johnson, M.P. (2010). Xanthophylls as modulators of membrane protein function. Arch Biochem Biophys *504*, 78-85.

Sarvikas, P., Hakala-Yatkin, M., Donmez, S., and Tyystjarvi, E. (2010). Short flashes and continuous light have similar photoinhibitory efficiency in intact leaves. J Exp Bot *61*, 4239-4247.

Satoh, K., and Yamamoto, Y. (2007). The carboxyl-terminal processing of precursor D1 protein of the photosystem II reaction center. Photosynth Res *94*, 203-215.

Serôdio, J., Vieira, S., Cruz, S., and Coelho, H. (2006). Rapid light-response curves of chlorophyll fluorescence in microalgae: relationship to steady-state light curves and non-photochemical quenching in benthic diatom-dominated assemblages. Photosynth Res *90*, 15.

Sharma, J., Panico, M., Shipton, C.A., Nilsson, F., Morris, H.R., and Barber, J. (1997). Primary structure characterization of the photosystem II D1 and D2 subunits. J Biol Chem *272*, 33158-33166.

Siaut, M., Heijde, M., Mangogna, M., Montsant, A., Coesel, S., Allen, A., Manfredonia, A., Falciatore, A., and Bowler, C. (2007). Molecular toolbox for studying diatom biology in *Phaeodactylum tricornutum*. Gene *406*, 23-35.

Silva, P., Thompson, E., Bailey, S., Kruse, O., Mullineaux, C.W., Robinson, C., Mann, N.H., and Nixon, P.J. (2003). FtsH Is involved in the early stages of repair of photosystem II in *Synechocystis* sp PCC 6803. Plant Cell *15*, 2152-2164.

Takahashi, S., and Murata, N. (2008). How do environmental stresses accelerate photoinhibition? Trends Plant Sci *13*, 178-182.

Tyystjärvi (2008). Photoinhibition of Photosystem II and photodamage of the oxygen evolving manganese cluster. Coordin Chem Rev *252*, 361-376.

Walters, R.G. (2005). Towards an understanding of photosynthetic acclimation. J Exp Bot *56*, 435-447.

White, A.J., and Critchley, C. (1999). Rapid light curves: A new fluorescence method to assess the state of the photosynthetic apparatus. Photosynth Res *59*, 10.

Wu, H., Cockshutt, A.M., McCarthy, A., and Campbell, D.A. (2011). Distinctive photosystem II photoinactivation and protein dynamics in marine diatoms. Plant Physiol *156*, 2184-2195.

Yamamoto, Y. (2001). Quality control of photosystem II. Plant Cell Physiol *42*, 121-128.

Yamamoto, Y., Aminaka, R., Yoshioka, M., Khatoon, M., Komayama, K., Takenaka, D., Yamashita, A., Nijo, N., Inagawa, K., Morita, N., *et al.* (2008). Quality control of photosystem II: impact of light and heat stresses. Photosynth Res *98*, 589-608.

Yamamoto, Y., Nishi, Y., Yamasaki, H., Uchida, S., and Ohira, S. (2004). Assay of photoinhibition of photosystem II and protease activity. Methods Mol Biol *274*, 217-227.

Yoshioka, M., and Yamamoto, Y. (2011). Quality control of Photosystem II: Where and how does the degradation of the D1 protein by FtsH proteases start under light stress? - Facts and hypotheses. J Photochem Photobiol B.

Yun, M.S., Lee, S.H., and Chung, I.K. (2010). Photosynthetic activity of benthic diatoms in response to different temperatures. J Appl Phycol *22*, 559-562.

Zehr, J.P., and Kudela, R.M. (2009). Ocean science: Photosynthesis in the open ocean. Science *326*, 945-946.

Zhang, L., and Aro, E.M. (2002). Synthesis, membrane insertion and assembly of the chloroplast-encoded D1 protein into photosystem II. FEBS Lett *512*, 13-18.

Zhu, S.H., and Green, B.R. (2010). Photoprotection in the diatom *Thalassiosira pseudonana*: role of LI818-like proteins in response to high light stress. Biochim Biophys Acta *1797*, 1449-1457.

ANNEXES

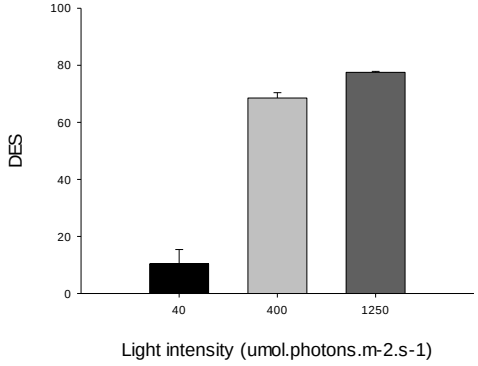

Annex I– DES at LL (low light, 40 µmol photons.m^{-2}.s^{-1}), HL high light, 1,250 µmol photons.m^{-2}.s^{-}and HL (high light, 1,250 µmol photons.m^{-2}.s^{-1}) and same 2 but with chloroplast protein synthesis inhibitor lincomycin (i).

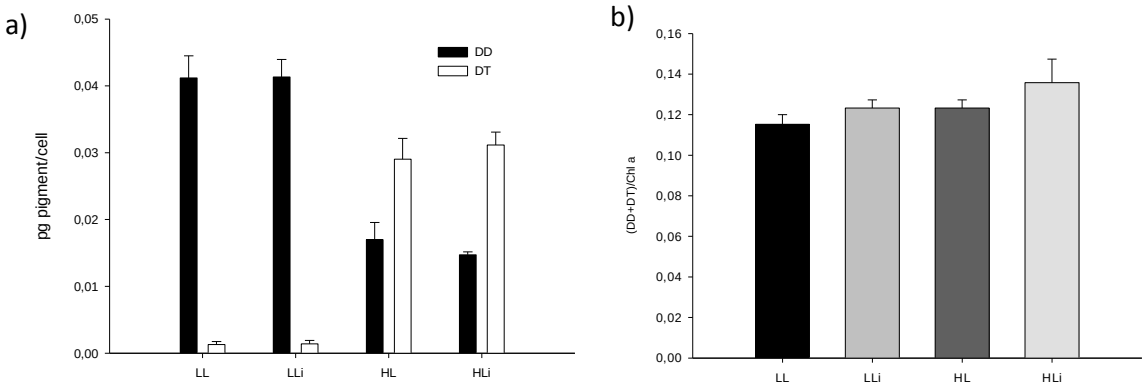

Annex II- DD and DT concentrationin*Phaeodactylum tricornutum*. 4 treatments tested: LL (low light, 40 µmol photons.m^{-2}.s^{-1}) and HL (high light, 1,250 µmol photons.m^{-2}.s^{-1}) and same 2 but with chloroplast protein synthesis inhibitor lincomycin (i) and; b)Chl *a*and xanthophylls relation [(DD+DT)/Chl *a*] in*Phaeodactylum tricornutum*. 4 treatments tested: LL (low light, 40 µmol photons.m^{-2}.s^{-1}) and HL (high light, 1,250 µmol photons.m^{-2}.s^{-1}) and same 2 but with chloroplast protein synthesis inhibitor lincomycin (i).

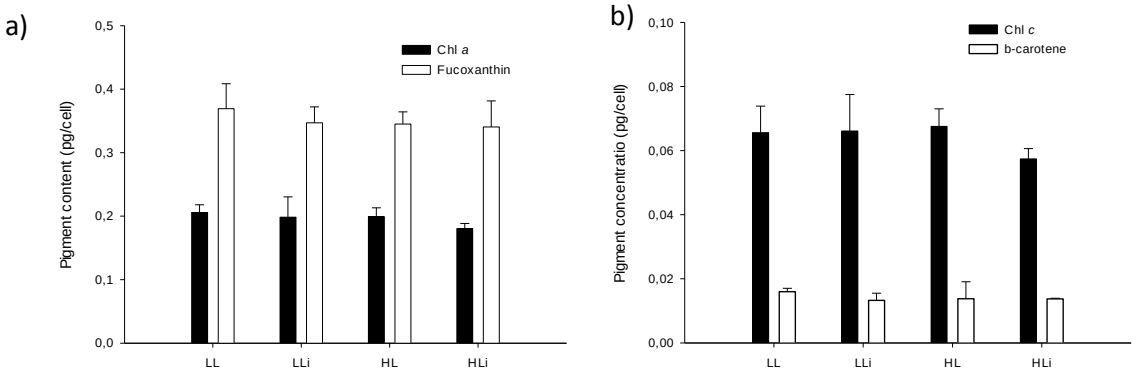

Annex III – a) Fucoxanthin and chlorophyll *a* contents in *Phaeodactylum tricornutum*. 4 treatments tested: LL (low light, 40 µmol photons.m^{-2}.s^{-1}) and HL (high light, 1,250 µmol photons.m^{-2}.s^{-1}) and same 2 but with chloroplast protein synthesis inhibitor lincomycin (i); b) β-carotene and chlorophyll *c* contents in *Phaeodactylum tricornutum*. 4 treatments tested: LL (low light, 40 µmol photons.m^{-2}.s^{-1}) and HL (high light, 1,250 µmol photons.m^{-2}.s^{-1}) and same 2 but with chloroplast protein synthesis inhibitor lincomycin (i).

Annex IV– Loss in photosystem II yield and respective fluorescence values for all 6 replicates of plastidial protein synthesis inhibited and non-inhibited samples of *Phaeodactylum tricornutum* 1 h after high light stress inducement of 1 h and 24 h of recovery in the dark at 15ºC:

	Inhibitor				Control			
	F_v/F_m	F_v/F_m' (1 h)	F_v/F_m' (24 h)	Loss of Y (%)	F_v/F_m	F_v/F_m' (1 h)	F_v/F_m' (24 h)	Loss of Y (%)
Replicates	0.630	0.320	0.337	49.2	0.647	0.548	0.542	15.3
	0.634	0.279	0.307	56.0	0.659	0.509	0.544	22.8
	0.629	0.417	0.418	33.7	0.659	0.531	0.533	19.4
	0.679	0.231	0.329	66.0	0.707	0.503	0.577	28.9
	0.671	0.282	0.381	58.0	0.725	0.478	0.569	34.1
Average	0.649	0.306	0.354	52.6	0.679	0.514	0.553	24.1
SD	0.022	0.069	0.045	12.1	0.034	0.027	0.019	7.5

Annex V – RLC parameters for all replicates:

	RLCs						
	Replicates	**Stress**	**α**	**$rETR_m$**	**β**	***Ek***	**r**
No lincomycin	I	Before	0,491	41,6	120,66	84,4	0,95
		After	0,179	38,1	47,83	213	0,95
	II	Before	0,491	43,1	116,29	87,6	0,93
		After	0,158	43	37,36	272,7	0,97
	III	Before	0,519	43,4	121,16	84,1	0,99
		After	0,158	43	37,36	272,7	0,97
	AVG	**Before**	**0,500**	**42,7**	**119,37**	**85,4**	
	SD		**0,016**	**1,0**	**2,68**	**1,9**	
	AVG	**After**	**0,165**	**41,4**	**40,85**	**252,8**	
	SD		**0,012**	**2,8**	**6,04**	**34,5**	
With lincomycin	I	Before	0,483	46,1	106,61	95,5	0,97
		After	0,189	33,7	57,11	178,5	0,98
	II	Before	0,607	34,3	180,32	56,5	0,96
		After	0,163	13,9	120,17	84,9	0,91
	III	Before	0,568	40,2	143,82	70,8	0,96
		After	0,183	21	88,75	114,9	0,95
	IV	Before	0,541	53,2	103,50	98,4	0,93
		After	0,204	25,5	81,41	125,2	0,97
	AVG	**Before**	**0,550**	**43,5**	**133,56**	**80,3**	
	SD		**0,052**	**8,1**	**36,15**	**20,1**	
	AVG	**After**	**0,185**	**23,5**	**86,86**	**125,9**	
	SD		**0,017**	**8,3**	**26,00**	**39,0**	